AD_____

Award Number: W81XWH-04-1-0235

TITLE: Involvement and Regulation of Heparanase in Prostate Cancer Progression

PRINCIPAL INVESTIGATOR: Dr. Michael Elkin

CONTRACTING ORGANIZATION: Hadassah Medical Organization
Jerusalem 91120
Israel

REPORT DATE: February 2007

TYPE OF REPORT: Final

PREPARED FOR: U.S. Army Medical Research and Materiel Command
Fort Detrick, Maryland 21702-5012

REPORT DOCUMENTATION PAGE

Form Approved
OMB No. 0704-0188

1. REPORT DATE *(DD-MM-YYYY)*	**2. REPORT TYPE**	**3. DATES COVERED** *(From - To)*
01-02-2007	Final	19 Jan 04 – 18 Jan 07

4. TITLE AND SUBTITLE
Involvement and Regulation of Heparanase in Prostate Cancer Progression

5a. CONTRACT NUMBER

5b. GRANT NUMBER
W81XWH-04-1-0235

5c. PROGRAM ELEMENT NUMBER

6. AUTHOR(S)
Dr. Michael Elkin

E-Mail: melkin@hadassah.org.il

5d. PROJECT NUMBER

5e. TASK NUMBER

5f. WORK UNIT NUMBER

7. PERFORMING ORGANIZATION NAME(S) AND ADDRESS(ES)

Hadassah Medical Organization
Jerusalem 91120
Israel

8. PERFORMING ORGANIZATION REPORT NUMBER

9. SPONSORING / MONITORING AGENCY NAME(S) AND ADDRESS(ES)
U.S. Army Medical Research and Materiel Command
Fort Detrick, Maryland 21702-5012

10. SPONSOR/MONITOR'S ACRONYM(S)

11. SPONSOR/MONITOR'S REPORT NUMBER(S)

12. DISTRIBUTION / AVAILABILITY STATEMENT
Approved for Public Release; Distribution Unlimited

13. SUPPLEMENTARY NOTES

14. ABSTRACT
Improvement in prostate cancer patient survival requires the identification of new therapeutic targets, based on a detailed understanding of the biologic mechanisms involved in metastatic dissemination and growth in bone and other target organs. Heparanase (HPSE) is a predominant mammalian enzyme that cleaves heparan sulfate, the main polysaccharide component of the extracellular matrix (ECM). The role of HPSE in sustaining the pathology of malignant tumors is being extensively studied during the last decade. The link between HPSE and prostate carcinoma progression remains less investigated and was disputed in recent publications, favoring or opposing involvement of the enzyme. Here we report that HPSE directly contributes to the prostate tumor take and growth in bone, as well as to its ability to metastasize to distant organs. Inhibitory strategies designed in the course of the research are hoped to develop into effective anti-cancer therapeutic modalities. Knowledge gained on the regulatory machinery of heparanase promoter is of high significance, as a part of general effort to define the exact molecular mechanisms of heparanase-driven prostate tumorigenesis. In summary, our results suggest that in prostate tumorigenesis HPSE may become important molecular marker in clinical decision-making process for prostate tumor patients, as well as a target for intervention.

15. SUBJECT TERMS
Heparanase, metastasis, bone homing, gene silencing

16. SECURITY CLASSIFICATION OF:			**17. LIMITATION OF ABSTRACT**	**18. NUMBER OF PAGES**	**19a. NAME OF RESPONSIBLE PERSON**
a. REPORT	**b. ABSTRACT**	**c. THIS PAGE**			**19b. TELEPHONE NUMBER** *(include area code)*
U	U	U	UU	43	USAMRMC

Standard Form 298 (Rev. 8-98)
Prescribed by ANSI Std. Z39.18

Table of Contents

	Page
Introduction……..	**4**
Body……..	**5**
Key Research Accomplishments……..	**14**
Reportable Outcomes……	**15**
Conclusion……	**16**
References……	**17**
Appendices……	**19**

INTRODUCTION

Prostate cancer is responsible for more gender-specific cancer-related deaths in men than any other cancer. The outcome of the disease is mainly determined by metastases, with the most frequent involvement of bone (90%) followed by lungs (46%), and to a less extent other soft viscera. Although curable if detected when confined to the prostate gland, the attempts at treatment have met with limited success once the disease has spread outside the prostate. Improvement in prostate cancer patient survival requires the identification of new therapeutic targets, based on a detailed understanding of the biologic mechanisms involved in metastatic dissemination and growth in bone and other target organs.

Heparanase is an endo-β-D-glucuronidase involved in cleavage of heparan sulfate (HS) and hence participates in ECM degradation and remodeling (1, 2). Heparanase activity has been traditionally correlated with the metastatic potential of tumor-derived cell types. Similarly, heparanase has been shown to facilitate cell invasion associated with autoimmunity, inflammation, and angiogenesis. Heparanase also releases angiogenic factors (i.e., bFGF, VEGF) from the ECM and thereby induces an angiogenic response *in vivo*. Preferential expression of heparanase was demonstrated in tissue specimens derived from several carcinoma types (3-6). A possible link between heparanase activity and prostate carcinoma progression was previously discussed as well, however, both observations supporting and opposing the enzyme contribution were reported.

The research summarized in the present report was undertaken to elucidate the biological and therapeutic significance of heparanase in prostate tumorigenesis. The series of experiments described below provide direct evidence for causal involvement of the heparanase enzyme in prostate tumor growth and metastasis. This report describes experimental systems and molecular tools developed in our laboratory, that allowed to investigate molecular regulatory mechanisms controlling heparanase expression in prostate cancer and to proceed to the recruitment of the most effective heparanase-inhibiting technologies toward development of new therapeutic modalities for prostate cancer.

BODY

Task # I. Involvement of heparanase, expressed by the tumor and stromal compartments, in prostate cancer progression.

i) heparanase overexpression in clinical samples of prostate carcinoma. Applying immunochemical staining of commercially available tissue microarrays with anti-heparanase antibody, we examined heparanase expression in the specimens of neoplastic and non-neoplastic prostate tissues. A scoring of the heparanase protein levels in the specimens was performed by an expert pathologist (scores: 0-no staining; 1-low heparanase staining; 2- high heparanase staining). Both the frequency and extent of heparanase overexpression were significantly enhanced in prostate carcinomas, as compared to benign lesions or normal prostate tissue (Figure. 1A). Heparanase protein was easily detected in 86% of prostate carcinoma specimens, while among non-malignant prostate tissue samples only 24% expressed detectable levels of heparanase (chi-square test $p < 0.0001$).

Proportion of tumors displaying higher levels of heparanase expression (score 2) was increased among the specimens scored with higher Gleason grade: 60% in the tumors scored with grade 5 (26 out of 43), versus 48% (22 out of 46) in the grade 4 tumors and 39% in grade 3 tumors (Spearman correlation coefficient =0.5215, Table 1). In a separate set of experiments, strong heparanase immunostaining was also observed in bone biopsy specimens from patients with metastatic prostate cancer (Fig. 1 B).

ii) Homozygous TRAMP mice were cross-mated with *hpa*-transgenic mice, according to our original experimental design; however only 5 double homozygous male mice were identified and all developed prostate tumors and dyed within 3-4 months after birth. TRAMP mice developed tumors at a much slower rate and survived for 8-12 months (Fig. 2). The corresponding female mice were not affected. It appears that the heparanase-rich tumor microenvironment of the *hpa*-transgenic mice supports tumor take, growth rate and metastasis, but the number of mice was too small and survival time too short for establishment of a double homozygous transgenic mice colony. Metastases formation was not evaluated, since only few mice were available and spared for establishment of a colony. Unfortunately, these mice dyed early and we were unable to obtain offspring. This, together with an almost complete loss of breeding capacity in our *hpa*-tg colony, cause us to abandon the TRAMP/ *hpa*-tg system and to focus on transplantable prostate

carcinoma models as an alternative approach (i.e., DU-145 primary tumors, CWR intracardiac injection, PC bone-to-lung metastasis).

iii). We found that mice intracardially injected with CWR cells genetically engineered to overexpress heparanase developed secondary tumors in distant sites vs. no detectable tumors in control CWR injected mice, as also reflected by the marked difference in survival time (Fig. 3). Nevertheless, bone metastasis per se could not be detected following intracardial inoculation of heparanase over-expressing cells (CWR, PC3). To address the role of heparanase enzyme in bone colonization, we adopted intraosseous PC3 prostate carcinoma model. PC3 cells expresses relatively low levels of endogenous heparanase (Fig. 4) and, upon intraosseous injection *in vivo*, produce osteolytic bone tumors that do not metastasize to the distant organs (7). Although prostate cancers metastases to bone are often osteoblastic, biochemical and histological studies clearly show that both bone resorption and formation occurs in the course of bone colonization by prostate carcinoma cells (8-11). Moreover, it was suggested that osteoblastic metastases form on trabecular bone at sites of previous osteoclastic resorption, and that such resorption is required for subsequent osteoblastic metastases formation (reviewed in (12)). Intraosseous PC3 tumor model is, therefore, suitable for studying the effects of heparanase on the degradative portion of prostate carcinoma-induced bone turnover and metastasis. In our experiments PC3 cells were stably transfected with empty pCDNA3 expressing vector (*Vo*), vector encoding for human heparanase (*Hpa*), or for a secreted form of heparanase (*Sp*) (13). Upon selection, more than 50 stable transfected clones were pooled (to avoid possible effects of insertional mutagenesis) and the cells were examined for heparanase enzymatic activity. As expected, increased enzymatic activity was detected in both PC3-Hpa and PC3-Sp cells, as compared to PC3-Vo cells (Fig. 4A). In accordance with the observed difference in heparanase enzymatic activity, elevated level of heparanase mRNA was observed in PC3-Hpa and PC3-Sp cells compared to a very low level in the PC3-Vo cells (Fig. 4A, inset). Heparanase activity was also detected in medium conditioned by PC3-Sp, but not PC3-Hpa or PC3-Vo transfectants (Fig. 4B), confirming secretion of the enzyme by PC3-Sp cells. Notably, expression of either the secreted or non-secreted heparanase conferred the same extent of increased ability to invade through Matrigel (a reconstituted basement membrane preparation) (Fig. 5 C, D).

To evaluate the effect of heparanase on intraosseous prostate tumor growth , PC3-Vo, PC3-Hpa and PC3-Sp cells were injected into the marrow cavity of the tibia of male SCID mice. On day 22 after injection PC3-Sp cells formed palpable tumors, while PC3-Vo and PC3-hpa cells formed tumors of detectable size only ten day later (Fig. 6A). The statistically significant difference between PC3-Sp and either PC3-Vo or PC3-hpa tumor size persisted throughout the duration of the experiment (at day 42 the calculated *p* value were 0.00461 and 0.02592, respectively, Fig. 6A). On day 23, six randomly selected mice from each group were sacrificed, their tibia removed and processed for histology. Histological examination of PC3-Sp bone tumors on day 23 post injection revealed that the bone tissue was almost completely replaced by a tumor that consisted of prostate carcinoma cells, occasionally mixed with bone tissue remnants. In contrast, in bones injected with either PC3-Vo or PC3-hpa cells, tumor masses of limited volume were found within the bone, the shape of the bone remained unchanged, no extensive bone destruction was noted and proper organization of the bone tissue was maintained on day 23 post injection (Fig. 6 B, C). To ensure that the observed effects were not a result of a difference in the proliferative capacity of PC3-Vo, PC3-Hpa, and PC3-Sp cells, we performed proliferation assay and found no statistically significant difference in proliferation rate between the 3 cell types (not shown).

Bone resorption appears to be an integral part of the hypothesized vicious cycle, through which prostate tumor cells stimulate bone turnover and bone turnover stimulates further tumor progression. Tumor cells secrete factors that promote the activity of osteoclasts, a unique cell type derived from hematopoetic stem cells and express a large number of highly specific enzymes involved in bone breakdown. As the bone matrix is destroyed, it releases growth factors and other stimulatory substances, capable of enhancing growth of prostate cancer cells that have colonized the bone (12). We found that bone metastases of prostate carcinoma overexpress heparanase (Fig. 1B). As outlined above, prostate carcinoma cells genetically engineered to overexpress heparanase provoked marked osteolytic response in mouse tibia model (Fig. 6 B, C). Interestingly, while no difference was found in the number of osteoclasts per millimeter of bone-tumor interface in mice injected with either control or heparanase –overexpressing PC-3 cells, increased amount of osteoclasts in the bone portion adjacent to tumor site was noted in mice injected with heparanase-overexpressing, as compared to control (Vo) PC-3 cells (Fig. 8). These findings, taken together with the fact that increased growth rate of secreted heparanase-expressing vs. control cells was observed in intraosseous, but not *in vitro* setting, suggest that

heparanase expression by prostate carcinoma cells may accelerate further bone colonization, by activating osteoclasts in the vicinity of the initial metastatic lesion, thus providing both space as well as growth –promoting bioactive molecules, capable of further stimulating bone colonization by prostate carcinoma cells. In light of the importance of secreted heparanase in bone colonization, we further investigated molecular mechanisms responsible for the enzyme secretion by prostate carcinoma cells. We found that the presence of mutated RAS protein (which is found in 20% of all prostate tumors) is responsible for heparanase secretion, while having no effect on the level of expression of heparanase gene (Fig. 9).

We examined the effect of heparanase on spontaneous metastatic dissemination of prostate carcinoma growing in bone. PC3-Vo, PC3-Hpa, or PC3-Sp cells, transfected with the luciferase gene (LUC), were injected into the tibia of SCID mice, and used the whole-body bioluminescent LUC imaging to monitor prostate tumor progression *in vivo.* Once LUC bioluminescence was first detected in the lungs of PC3-Hpa injected (Fig. 7A) but not PC-Vo-injected (not shown) animals (day 46 of the experiment), the mice in all three groups were euthanized, their lungs were stained with Bouin's solution and evaluated for the number of surface metastatic colonies. As demonstrated in figure 7, the lungs of mice injected with either PC3-Hpa or PC3-Sp cells were massively colonized by prostate carcinoma cells vs. no or very few metastatic nodules detected in the lungs of PC3-Vo injected mice.
Altogether these results demonstrate an ability of both non-secreted and secreted heparanase to contribute to prostate carcinoma metastasis, and emphasize the particular importance of the secreted enzyme in enhancement of bone-residing tumor growth.

Task # II. Regulation of heparanase promoter activity

i. Testosterone augments heparanase promoter activity in prostate cancer cells. Two putative androgen response elements (ARE) were identified in the 5' flanking region of the heparanase gene, located at positions –1540 and –1370 relative to the transcription initiation site. To investigate the effect of androgens on *hpa*-transcription, we constructed a DNA vector in which the *hpa*-promoter region (1.8 kb) containing the AREs is introduced in front of a luciferase reporter gene and demonstrated that this region is sufficient to support reporter gene expression in transiently transfected CWR cells. A 4-fold increase in transcriptional activity of the *hpa*-

promoter was obtained in AR positive CWR cells in response to a physiological concentration of testosterone (0.1 nM). In contrast, there was no effect in AR-negative DU145 cells. Androgen treatment also induced a 3-4-fold increase in heparanase mRNA expression in AR-positive (LNCaP, CWR) but not AR-negative prostate carcinoma cells, confirming the suggested androgen-dependent mechanism of heparanase induction.

ii. Heparanase promoter activity is regulated by p53. We revealed that wild type (wt), but not the mutant p53, is capable of direct binding to heparanase promoter and inhibiting its activity in several cell types, including prostate carcinoma (Fig. 10). Moreover, some mutant forms of p53 (i.e., p53-H175R) even activated heparanase promoter (Fig. 10).

In an attempt to investigate molecular mechanisms responsible for repression of heparanase transcription by p53, we tested whether trichostatin A (TSA), a potent and specific inhibitor of histone deacetylases (HDAC) (14), is able to prevent this repression (association between transcriptional repression by p53 and the recruitment of HDAC to the regulatory sequences of target genes, has been previously reported (15). Trichostatin A abolished the inhibitory effect of wt p53 on heparanase expression (Fig. 11), suggesting the involvement of histone deacetylation in negative regulation of the heparanase promoter. Altogether, our results indicate that the heparanase gene is regulated by p53 under normal conditions, while mutational inactivation of p53 during cancer development leads to induction of heparanase expression, providing a possible explanation for the frequent increase of heparanase levels observed in the course of prostate and other types of tumorigenesis. Our results implicate p53 in regulating heparanase expression not only in carcinoma cells *per se*, but also in fibroblasts. A marked stimulation of heparanase gene expression and enzymatic activity has been demonstrated in mouse embryonic fibroblasts derived from $p53^{-/-}$ mice. Moreover, transcriptional (siRNA) or functional (GSE 56) inactivation of p53 in telomerase-immortalized WI-38 human fibroblasts led to increased heparanase expression (Fig. 12 and (16)).

The critical importance in carcinogenesis of stromal elements (e.g., carcinoma-associated fibroblasts, CAFs) and their secreted factors is increasingly documented (17). Among other mechanisms, it was suggested that stromal cellular elements may contribute to the malignant potential of the tumor by producing heparanase (18). While normal fibroblasts lack detectable heparanase activity (19), and our unpublished observations), elevated levels of the heparanase

protein were detected in fibroblasts associated with deeply invading carcinoma (18). Recently, it becomes increasingly clear that inactivating mutations in p53 are responsible for the prostate tumor-supporting activities exerted by CAFs (20-22). Our results propose a molecular pathway through which CAFs, due to the loss of functional p53, may become an independent source of heparanase in the tumor vicinity, thus contributing to prostate carcinoma progression.

Task #3. Heparanase involvement in β-catenin nuclear trafficking and the down regulation of Wnt signaling. Our initial results have suggested that heparanase binds β-catenin and γ-catenin in the cytoplasm and nucleus of prostate cancer cells. In other experiments we have found inhibition of Wnt signaling, as well as down regulation of c-myc, in the heparanase-transfected vs. control cells. However, further attempts to evaluate heparanase/β-catenin interaction and its biological significance did not provide unequivocal and/or reproducible results, justifying further experimentation in this research direction.

Task # IV: Inhibitory strategies

i) EGFR-heparanase interaction: Role of the EGFR family, particularly ErbB-2, in the prostate tumorigenesis is well documented and EGFR-targeting was suggested to be of therapeutic relevance in prostate cancer. Studying effects of EGFR tyrosine kinase inhibitors on heparanase activity in human prostate cancer cell lines, we noticed that, unexpectedly, over expression of endogenous heparanase (Fig. 13), or addition of the exogenous enzyme (Fig. 14) to the cells induces EGFR phosphorylation. In an attempt to characterize a molecular mechanism of such an unexpected activity of heparanase protein, we found that enhanced EGFR phosphorylation upon heparanase over expression is Src-dependent (Fig. 15). Thus, heparanase-silencing strategies (see the last section of this report) may exert additional beneficial impact in prostate carcinoma treatment, acting to diminish EGFR effects.

ii). Low molecular weight glycol-split species of heparins: Analysis of a series of modified species of heparin led to the identification of several nonanticoagulant compounds that efficiently inhibit heparanase enzymatic activity while lacking additional, undesired activities of heparin (e.g., anticoagulation, release and activation of heparin-binding pro-angiogenic factors). A promising heparanase inhibitors are glycol-split heparin (compound ST1514) or N-acetylated

glycol-split heparin (compound G-4000), identified as most effective heparanase-inhibiting species of non-anticoagulant heparin, which inhibits the enzyme *in vitro* at nanomolar concentrations (0.02–0.1 nM, not shown). In our initial experiments we have used the B16-BL6 mouse melanoma experimental metastasis model to demonstrate anti-metastatic effects these compounds, (>90% inhibition of melanoma lung colonization, Fig. 16). The effectiveness of the glycol-split heparin for suppressing the biological activity of heparanase was also judged by the inhibitory effect of ST1514 administration in experimental model of heparanase-driven biological processes, such as DTH inflammation (23). During the last year of research, the attempt is being made to demonstrate anti-tumor effect of these compounds in prostate carcinoma in vivo models: G-4000 compound was administered both intraperitoneously, and, taking into account its relatively short half-life (~2 h), continuously (mini-osmotic pumps; 25 mg/kg/day). Although up to date no statistically significant effect on prostate tumor growth inhibition was detected, we feel that further experiments (which are underway), involving additional cell models and more effective delivery strategies (i.e., liposomes and other slow release systems) will eventually enable to demonstrate therapeutic benefit of the tested compound in prostate cancer, as it was already demonstrated in other tumor types.

iii) Hpa gene silencing *in vivo*, as an approach to: **i)** eliminate both enzymatic and non-enzymatic activities of heparanase; and **ii)** elucidate the role of host- and tumor-derived heparanase in cancer metastasis and angiogenesis

We prepared siRNAs directed against the human and mouse heparanase mRNAs and designed anti-mouse heparanase siRNA-expressing plasmid pSi and anti-human heparanase siRNA-expressing plasmid pSH1 (23, 24). Heparanase gene silencing approach is especially important in light of the recently discovered non-enzymatic functions of heparanase such as cell adhesion and survival signals (25, 26) — functions that may be integral part of cancer promotion by heparanase, but are not sensitive to the currently available inhibitors of heparanase enzymatic activity.

a. *Electroporation assisted delivery of siRNA.* We developed a reliable system for siRNA administration by *in vivo* electroporation of siRNA expressing vectors. To verify the effectiveness of this approach for suppressing the biological activity of heparanase *in vivo* we first utilized the skin DTH inflammation model, as a prototype of heparanase-driven biological

processes which enables quick and reliable monitoring of the inhibitory effect of siRNA administration (23). Following confirmation of heparanase-inhibiting ability of siRNA electroporation in vivo in the above-mentioned study, we further apply this approach for experimental PC treatment. We injected SCID mice intradermally with DU145 PC cells and, upon development of palpable tumors (~2-3 mm in diameter), electroporated the tumors with either mixture of anti-human and anti-mouse heparanase siRNA expressing plasmid, or control empty vector pSUPER. Treatment with heparanase siRNA resulted in augmented DU145 tumor regression, as compared to tumors treated with the control plasmid (Fig. 17). To test the local heparanase expression in siRNA-treated tumors and to ensure that electroporation of siRNA-expressing plasmids resulted in heparanase silencing throughout the *in vivo* experiment, we compared heparanase immunostaining in tissue sections of the DU145 tumors untreated, electroporated with empty pSUPER vector, or with the mixture of siRNA-expressing plasmids. Intense heparanase staining was observed in both untreated and pSUPER-electroporated tumors (Fig. 18 left, middle), vs. a very weak staining in pSi2/pSH1 electroporated tumors (Fig. 18 right). Decrease in a staining intensity in pSi2/pSH1 -electroporated group was evident in both mouse-derived (i.e., epidermis) and human-derived (i.e., tumor) cells, (Fig. 18 right), consistent with the administration of both pSi2 and pSH1 vectors.

Apart of exploration of the therapeutic potential of heparanase gene silencing for prostate cancer, siRNA tools enable to dissect the contributory role of tumor- vs. host-derived heparanase in prostate carcinoma progression. It is well established that cellular components of the tumor stroma (i.e., activated fibroblasts, immune and inflammatory cells, blood vessel cells) are actively involved in modulation and promotion of carcinoma growth (27). The siRNA approach, unlike enzymatic inhibitors, offers the opportunity to silence selectively either the mouse or human heparanase gene in experimental systems of human carcinoma growing in mouse host, since anti-mouse siRNA is unable to silence the human gene (Fig. 19) and vice versa. To evaluate the precise role of host- vs. tumor-derived heparanase in tumor growth, we treat the human PC tumor growing in mouse host with either anti-mouse siRNA, anti human siRNA, a mixture of the two plasmids, or empty vector alone. Utilizing this approach we compared both primary tumor growth rate and spontaneous metastasis in mice bearing intraosseous DU145 tumor, treated with either anti mouse or anti human siRNA, a mixture of the two plasmids, or control vector alone,

and found that both host- and tumor- derived heparanase are required for primary tumor growth, whereas tumor-derived enzyme is of primary importance for metastatic spread.

Table 1. Frequency and extent of HPSE expression in non-malignant and malignant prostate tissue samples

Condition	Normal			PIN			Grade 3			Grade 4			Grade 5		
HPA staining score	0	1	2	0	1	2	0	1	2	0	1	2	0	1	2
n	31	11	1	6	0	0	2	18	13	10	14	22	5	12	26
% per condition	72.1	25.6	2.3	100	0	0	6.1	54.5	39.4	21.7	30.4	47.8	11.6	27.9	60.5

KEY RESEARCH ACCOMPLISHMENTS.

i) Heparanase has been characterized as a promising molecular marker of prostate tumorigenesis, that may become important in clinical decision-making process for prostate cancer patients;

ii) direct evidences for causative involvement of the heparanase in both prostate tumor primary growth and metastasis were obtained, validating the potential of heparanase as a target for prostate tumor treatment;

iii) prostate tumors having elevated levels of secreted heparanase were shown to promote bone remodeling and resorption, boosting the promise for effective therapies, designed to block heparanase function, which may disrupt the early progression of bone-homing tumors.

iv) RAS-dependent mechanism, that may be responsible for heparanase secretion in a significant fraction of prostate tumors, has been described;

v) heparanase expression in prostate was found to be tightly regulated at the level of promoter activity. In particular, testosterone and p53 have been identified as critical determinants of heparanase promoter activation/suppression (respectively).

vi) Several antiheparanase inhibitory approaches were designed and tested in proof-of-concept *in vivo* settings:
- enzymatic inhibition approach: chemically modified species of heparin with increased heparanase-inhibiting ability but lacking other biological activities of normal heparin (i.e., anticoagulant, pro-angiogenic) that are irrelevant or undesirable in the case of anti-tumor drug development.
- gene-silencing approach: short inhibitory RNA (siRNA) characterized by increased stability and specificity of targeting.

REPORTABLE OUTCOMES.

Publications:

Baraz, L., Haupt, Y., Elkin, M., Peretz, T., and Vlodavsky, I. Tumor suppressor p53 regulates heparanase gene expression. Oncogene, 25, 3939-3947 (2006).

Edovitsky E, Lerner I, Zcharia E, Peretz T, Vlodavsky I, Elkin M. Role of endothelial heparanase in delayed-type hypersensitivity reaction. Blood, 2006 May 1;107(9):3609-16.

Lerner, I., Pikarsky, E ., Baraz, L., Edovitsky E., and Elkin, M . Function of heparanase enzyme in prostate tumorigenesis: potential for diagnosis and therapy. Cancer Research, under revision, 2007.

Abstracts & Presentations:

2005. Abstract: "Heparanase silencing averts tumor progression and inflammation", chosen for oral presentation at the 2005 AACR Annual Meeting (Anaheim, California). Presenter (E. Edovitsky) was awarded with AACR Scholar-in-Training Awards for Early-Career Scientists.

2006. Oral Presentation and Poster: **"**A Human Heparanase: Promising Target for Therapeutic Strategies in Prostate Cancer". AACR Special Conference "Innovations in Prostate Cancer", San-Francisco, CA, 2006. Presenter (Immanuel Lerner) was awarded with AACR Young Investigator Scholar Award

Funding applied for, based on work supported by this award:

Israel Cancer Research Fund postdoctoral fellowship (Lea Baraz) –Awarded (January 2005).

Israel Science Foundation Research Grant "Human heparanase: a promising target for therapeutic strategies in cancer"- Awarded (October 2006).

Degrees obtained that are supported by this award:

PhD degree –E. Edovitsky

Training supported by this award:

Training toward PhD degree – O. Kovalchik/I. Lerner

Postdoctoral training – R. Jaruss

CONCLUSIONS.

Improvement in prostate cancer patient survival requires the identification of new therapeutic targets, based on a detailed understanding of the biologic mechanisms involved in metastatic dissemination and growth in bone and other target organs. Our research focused on heparanase enzyme and characterization of its role in sustaining the pathology of prostate cancer. Involvement of heparanase in tumor progression is being studied during the last decade, and supported by numerous reports describing overexpression of the enzyme in malignant tumors of various origin. However, the relationship between heparanase and prostate carcinoma progression remains less unequivocal. The results obtained during the research period clearly demonstrate the involvement of heparanase in prostate tumorigenesis, as hypothesized in our original application. We report that heparanase directly contributes to the prostate tumor take and growth in bone, as well as to its ability to metastasize to distant organs. **So what**: We demonstrate that in prostate tumorigenesis heparanase may become important molecular marker in clinical decision-making process for prostate tumor patients, as well as a target for intervention. Inhibitory strategies designed in the course of the research are hoped to develop into effective anti-cancer therapeutic modalities. Knowledge gained on the regulatory machinery of heparanase promoter is of high significance, as a part of general effort to define the exact molecular mechanisms of heparanase-driven prostate tumorigenesis.

List of personnel receiving pay from the research effort:

Edovitsky E.

Aingorn E.

Atzmon R.

Jaruss R.

Kovalchik O.

Lerner I.

References

1. Parish, C. R., Freeman, C., and Hulett, M. D. Heparanase: a key enzyme involved in cell invasion. Biochim Biophys Acta, *1471:* M99-108., 2001.
2. Vlodavsky, I. and Friedmann, Y. Molecular properties and involvement of heparanase in cancer metastasis and angiogenesis. J Clin Invest, *108:* 341-347., 2001.
3. Gohji, K., Okamoto, M., Kitazawa, S., Toyoshima, M., Dong, J., Katsuoka, Y., and Nakajima, M. Heparanase protein and gene expression in bladder cancer. J Urol, *166:* 1286-1290., 2001.
4. Maxhimer, J. B., Pesce, C. E., Stewart, R. A., Gattuso, P., Prinz, R. A., and Xu, X. Ductal carcinoma in situ of the breast and heparanase-1 expression: A molecular explanation for more aggressive subtypes. J Am Coll Surg, *200:* 328-335, 2005.
5. Nobuhisa, T., Naomoto, Y., Ohkawa, T., Takaoka, M., Ono, R., Murata, T., Gunduz, M., Shirakawa, Y., Yamatsuji, T., Haisa, M., Matsuoka, J., Tsujigiwa, H., Nagatsuka, H., Nakajima, M., and Tanaka, N. Heparanase expression correlates with malignant potential in human colon cancer. J Cancer Res Clin Oncol, *131:* 229-237, 2005.
6. Tang, W., Nakamura, Y., Tsujimoto, M., Sato, M., Wang, X., Kurozumi, K., Nakahara, M., Nakao, K., Nakamura, M., Mori, I., and Kakudo, K. Heparanase: a key enzyme in invasion and metastasis of gastric carcinoma. Mod Pathol, *15:* 593-598, 2002.
7. Sobel, R. E. and Sadar, M. D. Cell lines used in prostate cancer research: a compendium of old and new lines--part 2. J Urol, *173:* 360-372, 2005.
8. Akimoto, S., Furuya, Y., Akakura, K., and Ito, H. Comparison of markers of bone formation and resorption in prostate cancer patients to predict bone metastasis. Endocr J, *45:* 97-104, 1998.
9. Percival, R. C., Urwin, G. H., Harris, S., Yates, A. J., Williams, J. L., Beneton, M., and Kanis, J. A. Biochemical and histological evidence that carcinoma of the prostate is associated with increased bone resorption. Eur J Surg Oncol, *13:* 41-49, 1987.
10. Revilla, M., Arribas, I., Sanchez-Chapado, M., Villa, L. F., Bethencourt, F., and Rico, H. Total and regional bone mass and biochemical markers of bone remodeling in metastatic prostate cancer. Prostate, *35:* 243-247, 1998.
11. Garnero, P., Buchs, N., Zekri, J., Rizzoli, R., Coleman, R. E., and Delmas, P. D. Markers of bone turnover for the management of patients with bone metastases from prostate cancer. Br J Cancer, *82:* 858-864, 2000.
12. Keller, E. T. and Brown, J. Prostate cancer bone metastases promote both osteolytic and osteoblastic activity. J Cell Biochem, *91:* 718-729, 2004.
13. Goldshmidt, O., Zcharia, E., Aingorn, H., Guatta-Rangini, Z., Atzmon, R., Michal, I., Pecker, I., Mitrani, E., and Vlodavsky, I. Expression pattern and secretion of human and chicken heparanase are determined by their signal peptide sequence. J Biol Chem, *276:* 29178-29187, 2001.
14. Yoshida, M., Kijima, M., Akita, M., and Beppu, T. Potent and specific inhibition of mammalian histone deacetylase both in vivo and in vitro by trichostatin A. J Biol Chem, *265:* 17174-17179, 1990.
15. Murphy, M., Ahn, J., Walker, K. K., Hoffman, W. H., Evans, R. M., Levine, A. J., and George, D. L. Transcriptional repression by wild-type p53 utilizes histone deacetylases, mediated by interaction with mSin3a. Genes Dev, *13:* 2490-2501, 1999.

16. Baraz, L., Haupt, Y., Elkin, M., Peretz, T., and Vlodavsky, I. Tumor suppressor p53 regulates heparanase gene expression. Oncogene, *25:* 3939-3947, 2006.
17. Bhowmick, N. A. and Moses, H. L. Tumor-stroma interactions. Curr Opin Genet Dev, *15:* 97-101, 2005.
18. Friedmann, Y., Vlodavsky, I., Aingorn, H., Aviv, A., Peretz, T., Pecker, I., and Pappo, O. Expression of heparanase in normal, dysplastic, and neoplastic human colonic mucosa and stroma. Evidence for its role in colonic tumorigenesis. Am J Pathol, *157:* 1167-1175, 2000.
19. Nadav, L., Eldor, A., Yacoby-Zeevi, O., Zamir, E., Pecker, I., Ilan, N., Geiger, B., Vlodavsky, I., and Katz, B. Z. Activation, processing and trafficking of extracellular heparanase by primary human fibroblasts. J Cell Sci, *115:* 2179-2187., 2002.
20. Olumi, A. F., Grossfeld, G. D., Hayward, S. W., Carroll, P. R., Tlsty, T. D., and Cunha, G. R. Carcinoma-associated fibroblasts direct tumor progression of initiated human prostatic epithelium. Cancer Res, *59:* 5002-5011, 1999.
21. Tuxhorn, J. A., McAlhany, S. J., Dang, T. D., Ayala, G. E., and Rowley, D. R. Stromal cells promote angiogenesis and growth of human prostate tumors in a differential reactive stroma (DRS) xenograft model. Cancer Res, *62:* 3298-3307, 2002.
22. Hill, R., Song, Y., Cardiff, R. D., and Van Dyke, T. Selective evolution of stromal mesenchyme with p53 loss in response to epithelial tumorigenesis. Cell, *123:* 1001-1011, 2005.
23. Edovitsky, E., Lerner, I., Zcharia, E., Peretz, T., Vlodavsky, I., and Elkin, M. Role of endothelial heparanase in delayed-type hypersensitivity. Blood, *107:* 3609-3616, 2006.
24. Edovitsky, E., Elkin, M., Zcharia, E., Peretz, T., and Vlodavsky, I. Heparanase gene silencing, tumor invasiveness, angiogenesis, and metastasis. J Natl Cancer Inst, *96:* 1219-1230, 2004.
25. Goldshmidt, O., Zcharia, E., Cohen, M., Aingorn, H., Cohen, I., Nadav, L., Katz, B. Z., Geiger, B., and Vlodavsky, I. Heparanase mediates cell adhesion independent of its enzymatic activity. Faseb J, *17:* 1015-1025, 2003.
26. Zetser, A., Bashenko, Y., Miao, H. Q., Vlodavsky, I., and Ilan, N. Heparanase affects adhesive and tumorigenic potential of human glioma cells. Cancer Res, *63:* 7733-7741, 2003.
27. Mueller, M. M. and Fusenig, N. E. Friends or foes - bipolar effects of the tumour stroma in cancer. Nat Rev Cancer, *4:* 839-849, 2004.

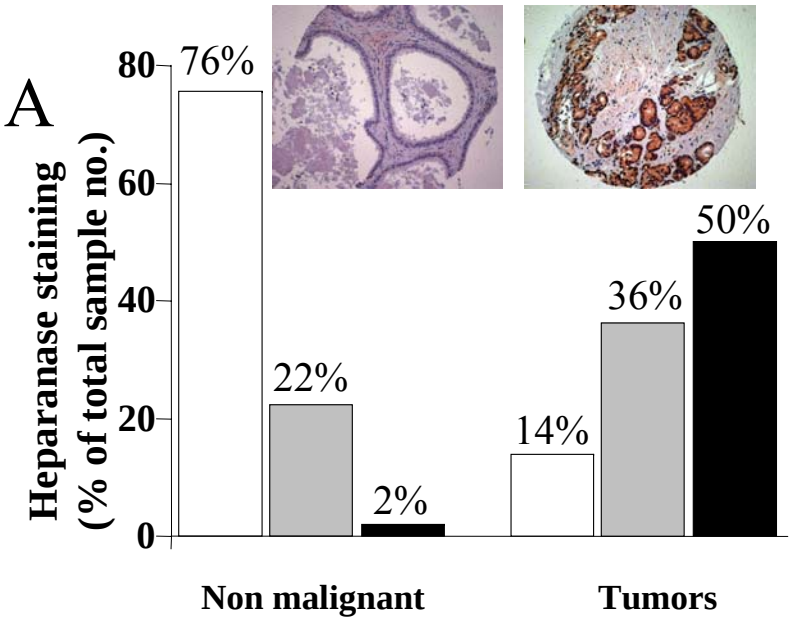

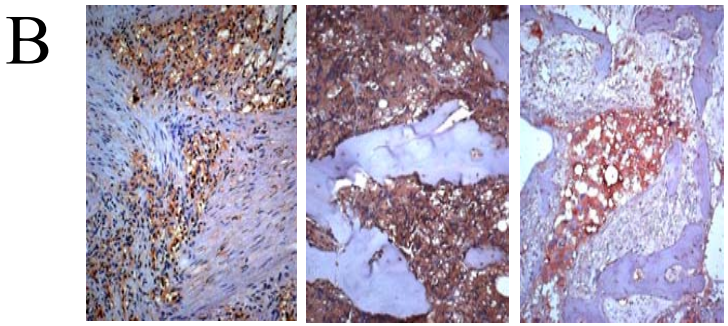

Figure 1. A. Tissue microarray analysis reveals preferential expression of HPSE in human prostate cancer. 171 specimens of neoplastic and non-neoplastic prostate tissues were stained with anti-HPSE antibody 733. Specimens were then graded according to HPSE staining intensity (white bars: no staining; grey bars: medium staining; black bars: high staining). Chi-squared analysis confirmed highly statistically significant ($p < 0.0001$) 3-fold higher prevalence of HPSE overexpression in prostate carcinomas vs. non-cancerous prostatic tissue. In addition, specimens were graded according to Gleason score, and strong positive correlation between tumor grade and the extent of HPSE expression was found (Spearman rank correlation coefficient = 0.5215; Table 1). **Inset:** Representative images of HPSE immunostaining in prostate tissue microarray specimens (non-neoplastic – *left;* carcinoma, Gleason grade 3 - *right*) Magnification X100. **B.** HPSE immunostaining of a bone biopsy specimen from the patients with metastatic prostate cancer.

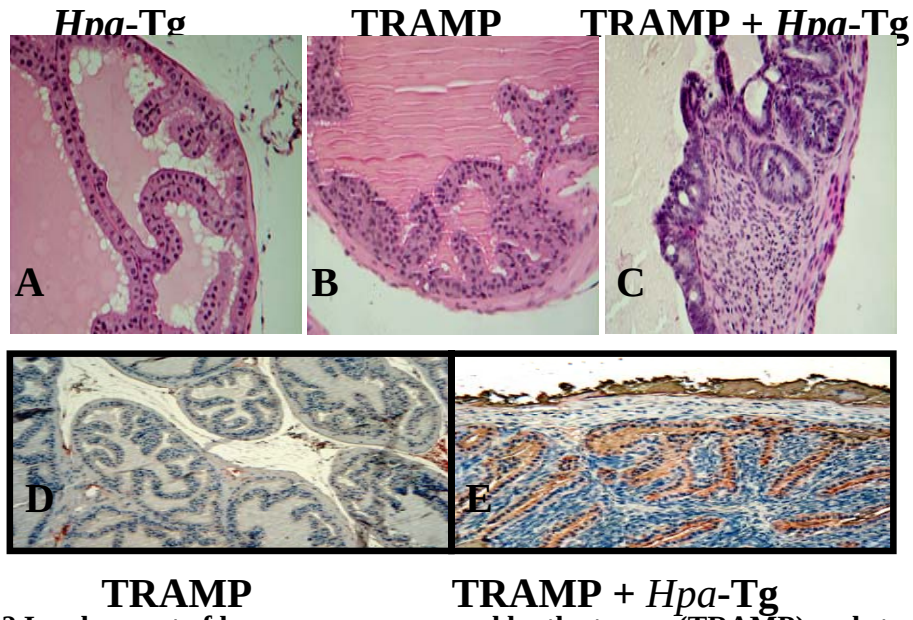

Figure 2 Involvement of heparanase, expressed by the tumor (TRAMP) and stromal (*hpa*-tg) compartments, in prostate cancer progression. Transgenic mice over-expressing heparanase (*Hpa*-tg) were cross-mated with TRAMP mice. Double homozygous male mice were identified by PCR using primers specific for TRAMP and heparanase. Cross-mating accelerated tumor formation and induced a pronounced stromal response (C). Over-expression of heparanase (immunostaining) is noted in the prostate epithelium of the cross-mated mice (E).

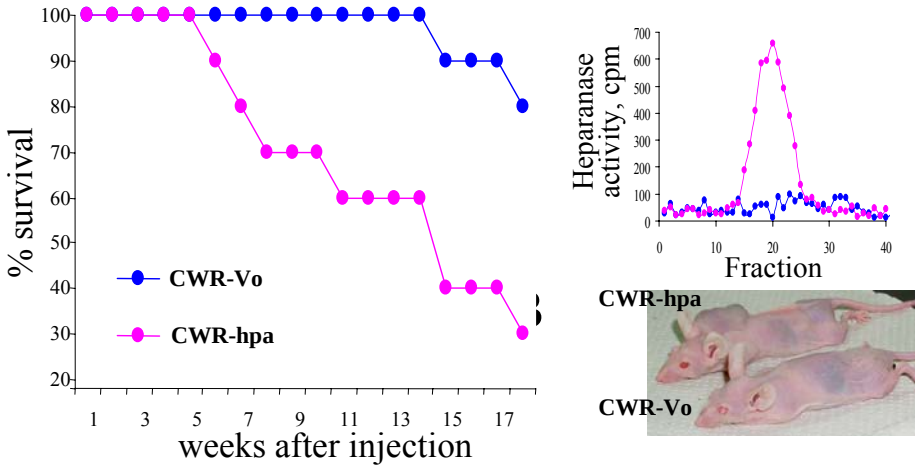

Figure 3. Balb/nude male mice received an intracardiac injection of CWR cells transfected with *Hpa*-pcDNA plasmid (CWR-*hpa*) or vector alone (CWR-Vo) High heparanase activity has been detected in CWR-*hpa*, but not in CWR-Vo cells (right, top). Mice injected with CWR-*hpa* cells developed secondary tumors in distant sites vs. no detectable tumors in CWR-Vo injected mice (right, bottom), reflected by a marked difference in survival time (left).

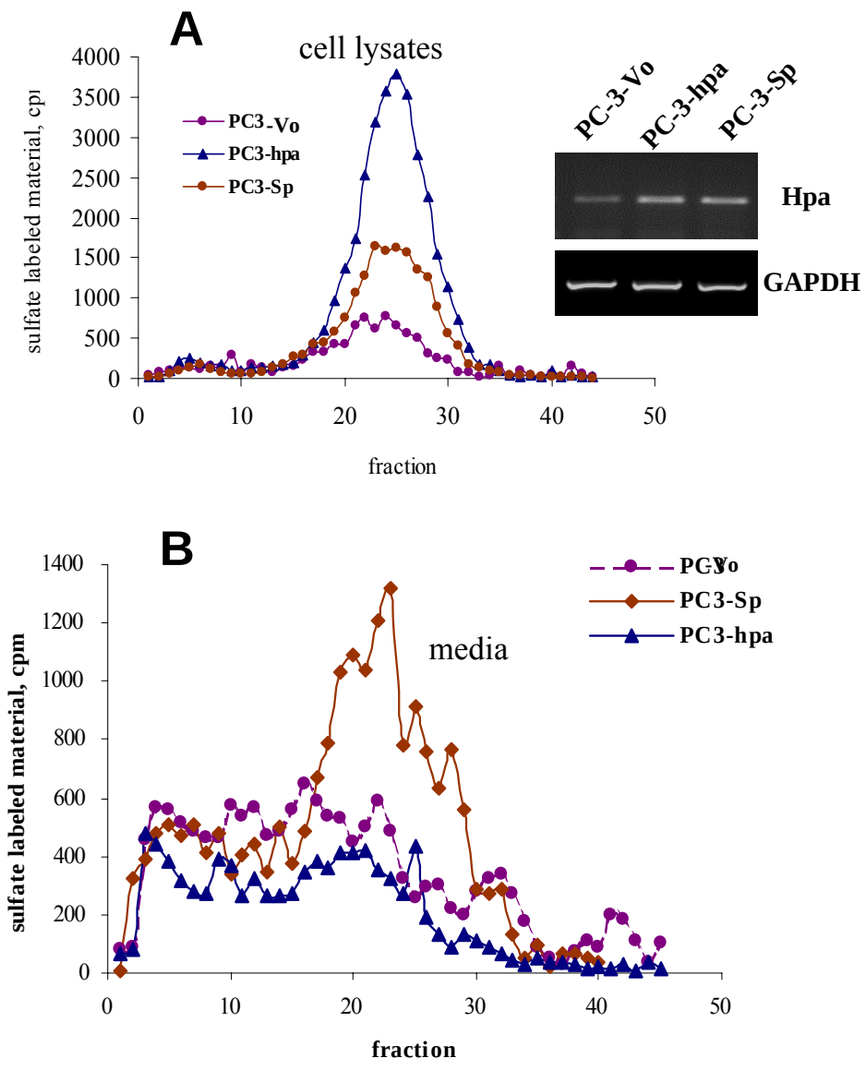

Figure 4. Heparanase enzymatic activity in transfected PC3 cells . **A**. PC3 cells stably transfected with empty vector (PC3-Vo), vector encoding human heparanase (PC3-hpa), or vector encoding a secreted form of heparanase (PC3-Sp) were lysed and tested for heparanase enzymatic activity. RNA was isolated from the 3 stable transfected cell types and subjected to RT-PCR for heparanase and GAPDH (control) (right, top). **B**. Heparanase enzymatic activity in medium conditioned by PC3-Vo, PC3-Sp and PC3-hpa cells.

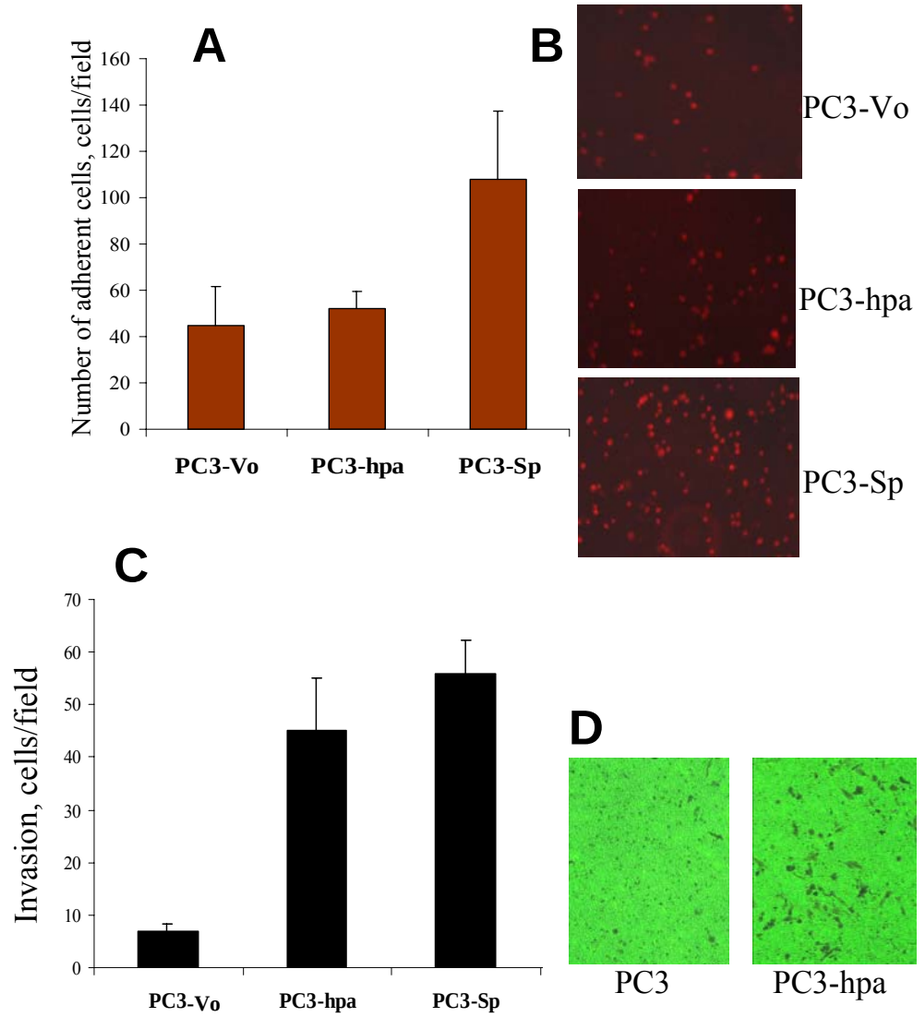

Figure 5. ***In-vitro*** **adhesion and invasion of heparanase transfected PC-3 cells. A**, **B.** PC3-Vo, PC3-Sp and PC3-hpa cells were tested for their ability to firmly adhere to bovine aortic endothelial cells (BAEC). Secreted heparanase (PC3-Sp) increases PC-3 adhesion to BAEC . **C, D**. Matrigel invasion assay. PC-3 cells transfected with human heparanase(PC3-hpa) or with secreted heparanase (PC3-Sp) exhibit a marked increase in cell invasion as compared to mock transfected PC3 cells.

Figure 6. **Over-expression of heparanase accelerates prostate tumor formation and growth. A**. PC3 cells stably transfected with empty vector (PC3-Vo), vector encoding heparanase (PC3-hpa), or secreted form of heparanase (PC3-Sp) were injected into the right tibia of SCID mice. Tumor size was monitored for 6.5 weeks.

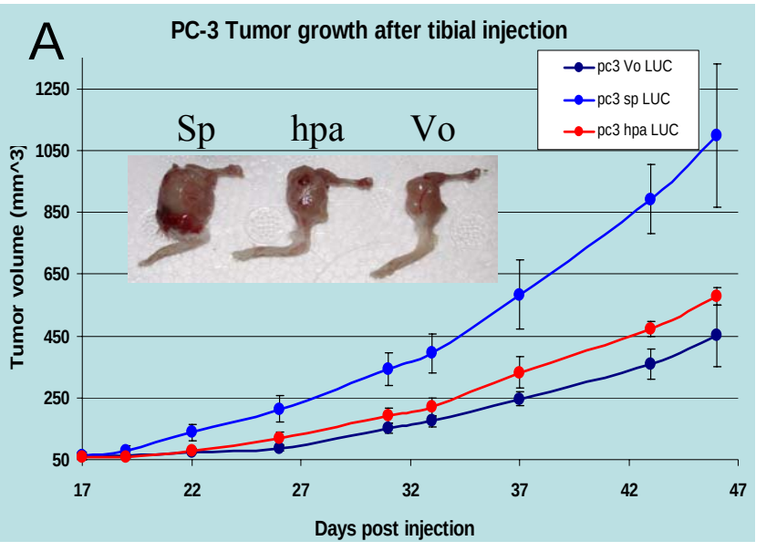

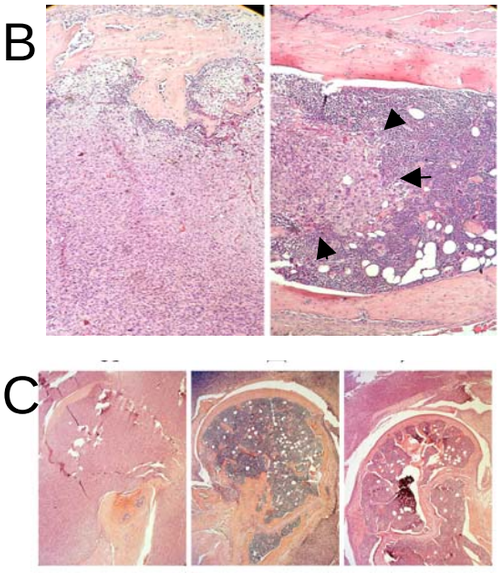

Inset: representative tumors, growing in mouse tibia on day 46 of experiment. **B, Left.** Histological examination of PC3-Sp bone tumors on day 23 post injection: the bone tissue is almost completely replaced by a tumor that consists of prostate carcinoma cells, occasionally admixed with bone tissue remnants. In bones injected with either PC3-Vo (not shown) or PC3-hpa (**B, Right**) cells, tumor masses of limited volume were found within the bone marrow (arrows), but the size of the bone has not changed. No bone destruction was noted and proper organization of the bone tissue was observed. **C**. Osteolytic effect of PC3-Sp (left), but not PC3-Hpa or PC3-Vo (middle, right) tibial tumors on the adjacent femur epiphyses. Tissue samples were collected on day 23 post injection, processed for histology and stained with H&E. Note nearly full replacement of epiphyses tissue by the PC3-Sp tumor cells (left).

Figure 7. **Over-expression of heparanase increases pulmonary metastasis in SCID mice**. PC3-Vo, PC3-Hpa and PC3-Sp cells, stably co-transfected with LUC expressing vector, were injected into the right tibia of SCID mice. **A.** 46 days post injection, when the presence of lung metastases was detected in the mice injected with either PC-3-*Hpa* or PC-3-*Sp*, but not PC-3-Vo cells by real time *in-vivo* bioluminescence imaging, all the mice were euthanized, and their lungs were fixed and examined for the number of carcinoma colonies on the lung surface. **B.** Gross appearance of lungs of mice injected with PC3-Vo (top), PC3-Hpa (middle) and PC3-Sp (bottom) cells. **C.** Bars represent the mean number of colonies per lung from 5 mice. Error bars show SEM. Statistically significant difference in number of colonies per lung was observed between PC3-Vo and either PC3-Sp ($P=0.019$), or PC3-hpa ($P=0.0413$) injected mice.

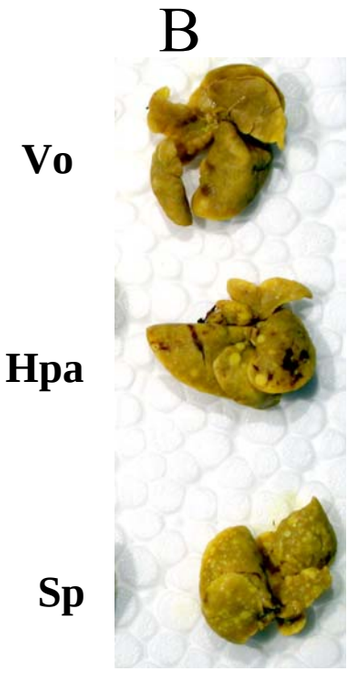

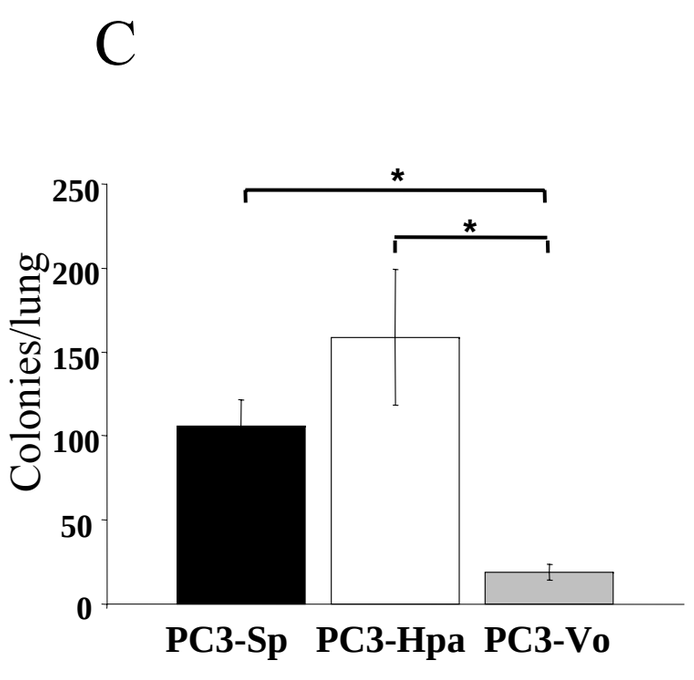

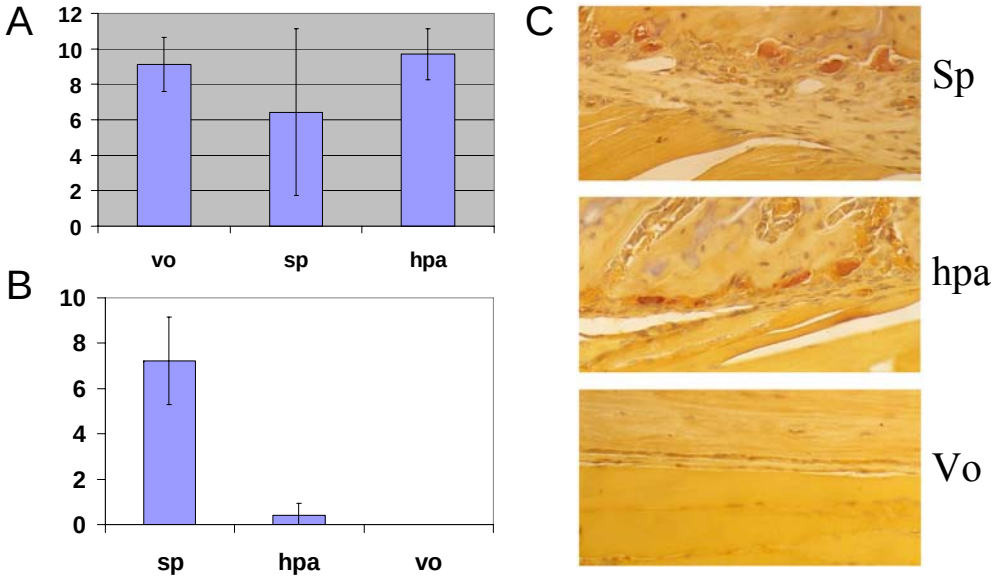

Figure 8. Histological sections of tissue specimens obtained from tumors formed by PC3-Vo, PC3-Hpa, and PC3-Sp cells were stained for TRAP, to visualize osteoclasts. **A**. No difference in the number of osteoclasts per millimeter of bone-tumor interface was found in mice injected with either control or heparanase –overexpressing PC-3 cells. **B, C**. Increased amount of osteoclasts in the bone portion adjacent to tumor site in mice injected with heparanase-overexpressing, as compared to control (Vo) PC-3 cells.

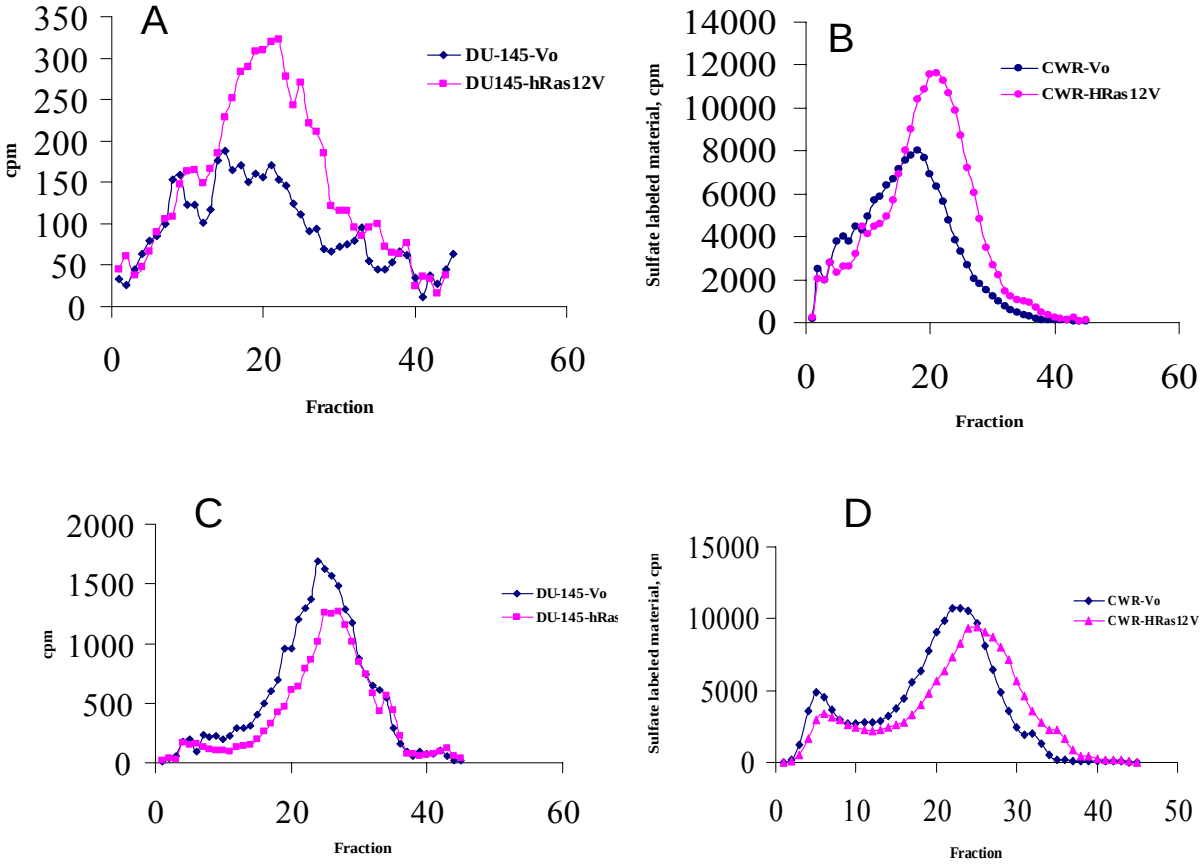

Figure 9. **Mutated RAS protein is responsible for heparanase secretion, without affecting the expression of heparanase gene.** CWR and DU-145 cells were transduced with pBABE-puro vector expressing oncogenic Ras, bearing point mutation G12Vor with control vector Vo. Heparanase activity in cell lysates was not changed as a result of mutant Ras overexpression C and D) . In contrast, heparanase secretion was markedly increased in RAS-G12V transduced cells (A and B). This increase was not due to elevated heparanase transcription as measured by RT-PCR and luciferase assay (not shown).

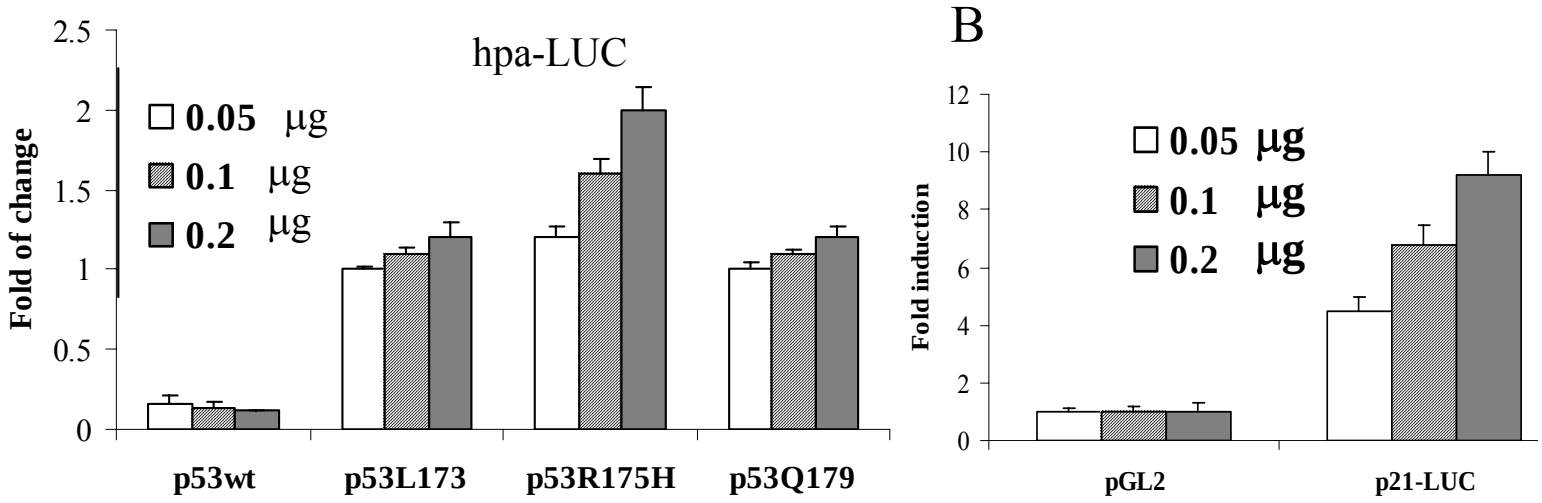

Figure 10. Effect of wt and mutated p53 on heparanase promoter activity. **A**. Dose-dependent repression of heparanase promoter activity by wt, but not mutant p53. p53-negative human osteosarcoma SaoS-2 cells were co-transfected with a 0.05 μg luciferase reporter gene driven by the heparanase promoter (Hpse-LUC) and with increasing amounts (0.05, 0.1 and 0.2 μg/well) of vectors encoding for wt or one of the three mutated p53 variants, commonly found in human cancer. Expression of wt p53 in SaoS-2 cells led to a dose-dependent decrease in heparanase promoter activity, as measured by the luciferase assay, reaching ~9-fold reduction in cells co-transfected with 0.2 μg of wt-p53 expressing plasmid. In contrast, none of the three tested p53 mutants displayed any repression ability. Moreover, one of the p53 mutant variants, demonstrated a slight (up to 2-fold) but consistently reproducible activation of heparanase promoter at the highest concentration.The graph represents the fold difference ±SD, as compared to control (SaoS-2 cells transfected with empty pcDNA3 vector only). Three independent experiments were performed in quadruplicates. **B.** Wt p53 does not affect SV40 promoter activity and activates the p21 promoter (p21-LUC). The experiment was performed as in A, except that pGL2 or p21-LUC plasmids, instead of Hpse-LUC, were co-expressed with increasing amounts of the wt p53 protein.

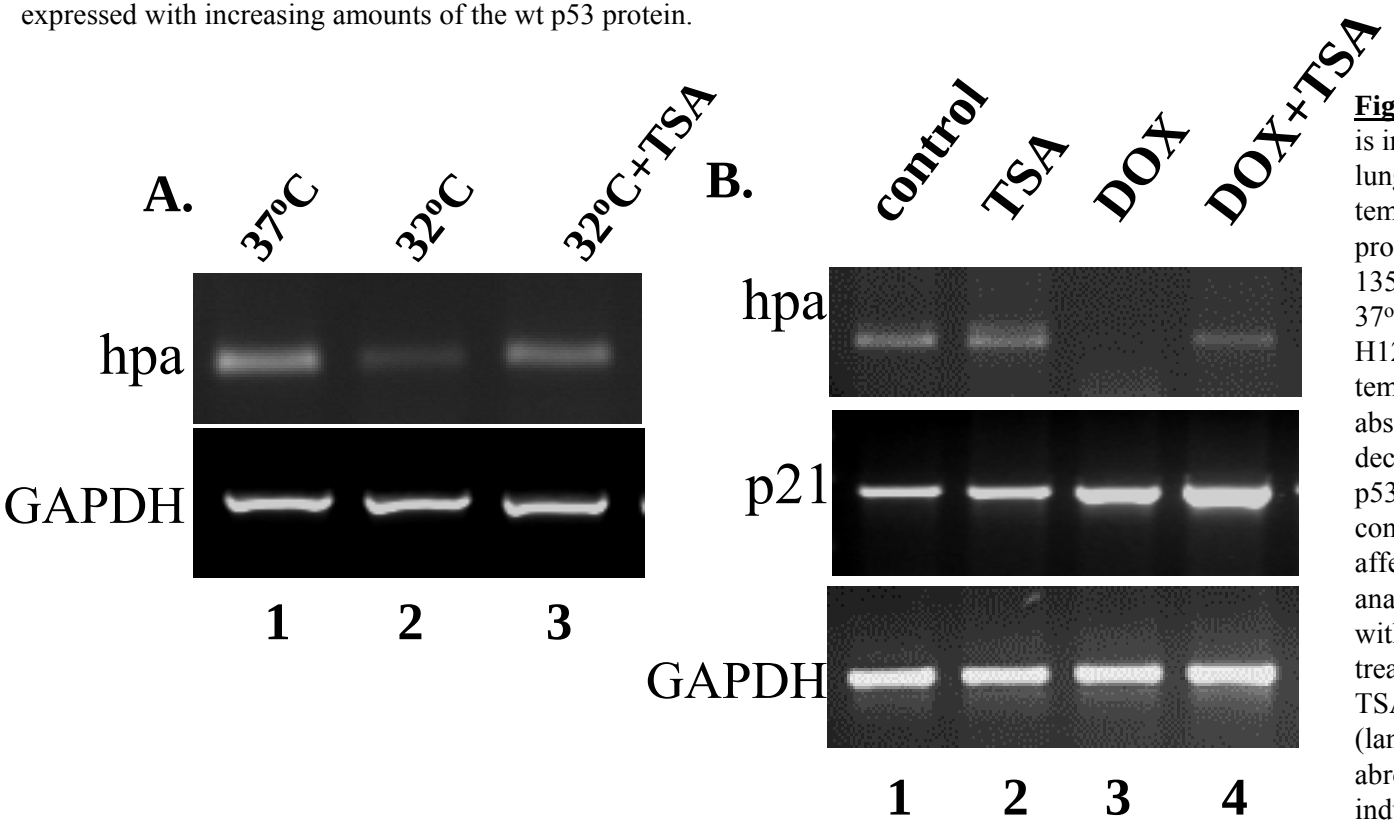

Figure 11. **A.** Transcriptional repression of heparanase by p53 is inhibited by the HDAC inhibitor TSA in p53-negative H1299 lung adenocarcinoma cells, stably transfected with a temperature sensitive Val135 mutant form of p53. This mutant protein contains a substitution from alanine to valine at position 135, which possesses wild-type p53 activity at 32°C, but not at 37°C. **A**. RT-PCR analysis of heparanase mRNA levels in H1299Val135 cells at 37°C (lane 1, mutant p53) and following temperature shift to 32°C for 24 h (wt p53 activity) in the absence (lane 2) or presence (lane 3) of 100nM TSA. The decrease of heparanase mRNA due to the temperature shift and p53 induction is largely reversed by incubation with TSA. In contrast, the level of housekeeping gene (GAPDH) is not affected by temperature shift or TSA treatment. **B.** RT-PCR analysis of heparanase levels in MCF-7 cells treated for 6 h with 1 μg/ml DOX, an inducer of p53, indicates that DOX treatment leads to repression of heparanase levels (lane 3). TSA treatment alone does not repress heparanase expression (lane 2). Repression of heparanase by DOX treatment is abrogated by TSA treatment)100 nM, lane 4). p21 level is induced as a result of DOX treatment and p53 activation (lanes 3 and 4), but is not affected by TSA treatment alone (lane 2).

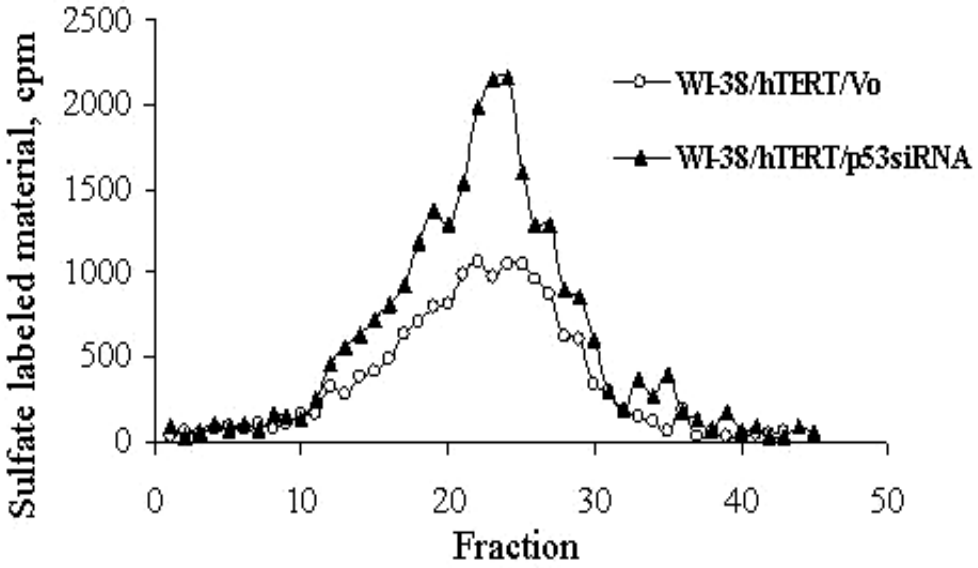

Figure 12. siRNA-mediated silencing of p53 elevates heparanase expression. WI-38/hTERT cells (1x106), infected with either lentiviral vector containing p53siRNA (▲) or control vector (○) were lysed 3 days post infection, normalized for equal protein, and cell lysates were tested for heparanase enzymatic activity. **Inset**. Heparanase (Hpa) mRNA expression. RNA was isolated 72 h post infection, reverse transcribed to cDNA and subjected to comparative semiquantitative PCR.

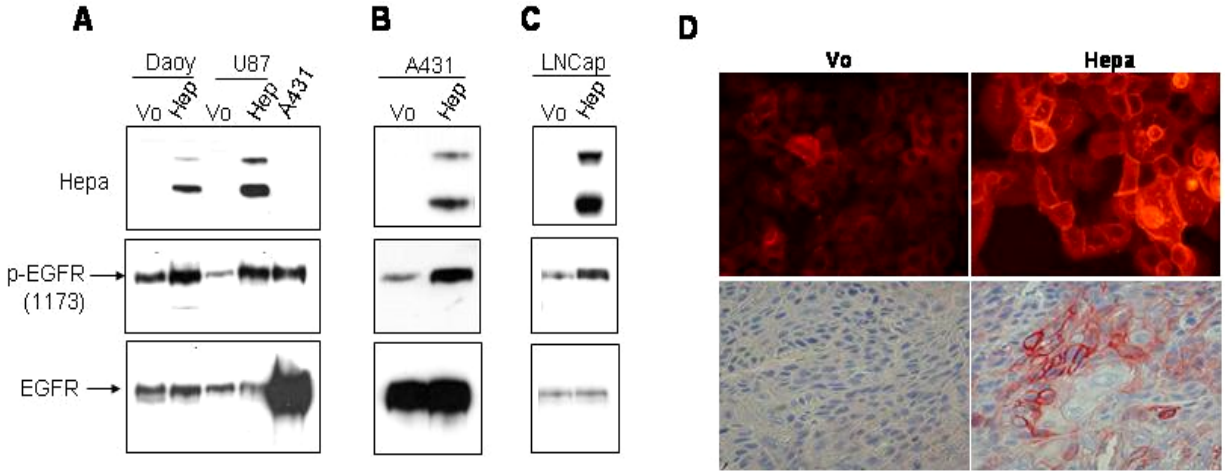

Figure 13. Heparanase over expression induces EGFR phosphorylation. **A-C**. Immunoblotting. Control (Vo) and heparanase transfected Daoy, U87 (A), A431 (B) and LnCAP (C) cell lysates were immunoblotted with anti-heparanase (upper panels), anti-phospho-EGFR (middle panels) and anti-EGFR (lower panels) antibodies. Note enhanced EGFR phosphorylation upon heparanase over expression. **D**. Immunostaining. Control, Vo, and heparanase transfected A431 cells (upper panels) and tumor xenografts sections (lower panels) were stained with anti-phospho-EGFR.

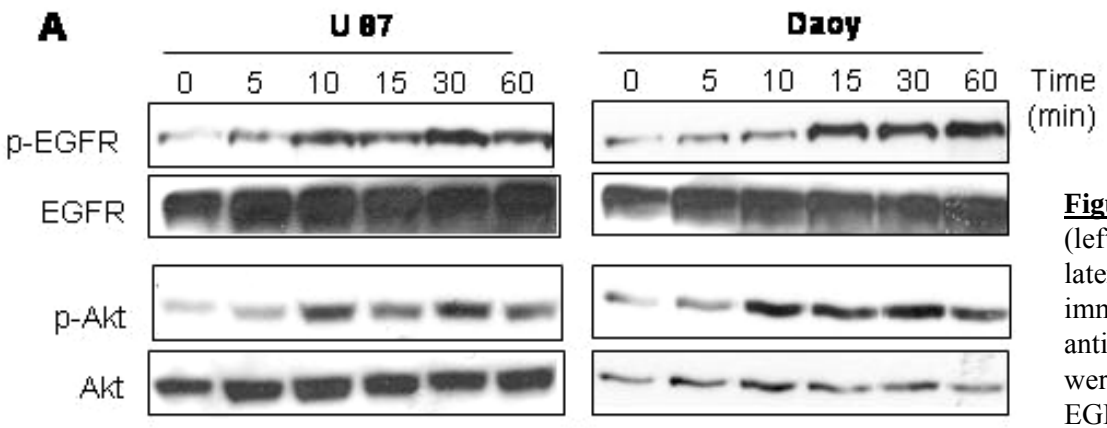

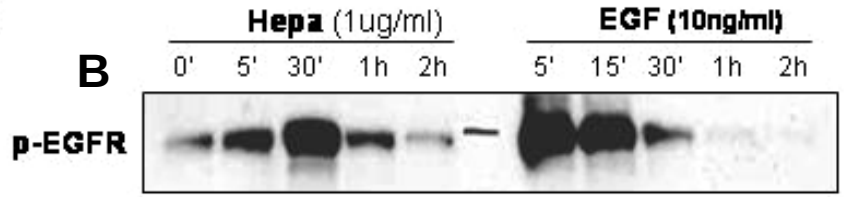

Figure 14. Exogenous addition of heparanase induces EGFR phosphorylation. **A**. U87 (left) and Daoy (right) cells were incubated without (0) or with recombinant purified latent 65 kDa heparanase (1 µg/ml) for the time indicate, and total cell lysates were immunoblotted with anti-phospho-EGFR (upper panels), anti-EGFR (second panels), anti-phospho-Akt (third panels) and anti-Akt (bottom panels) antibodies. **B**. U87 cells were left untreated (0) or incubated for the time indicated with heparanase (1µg/ml) or EGF (10ng/ml), and cell lysates were immunoblotted with anti-phospho-EGFR.

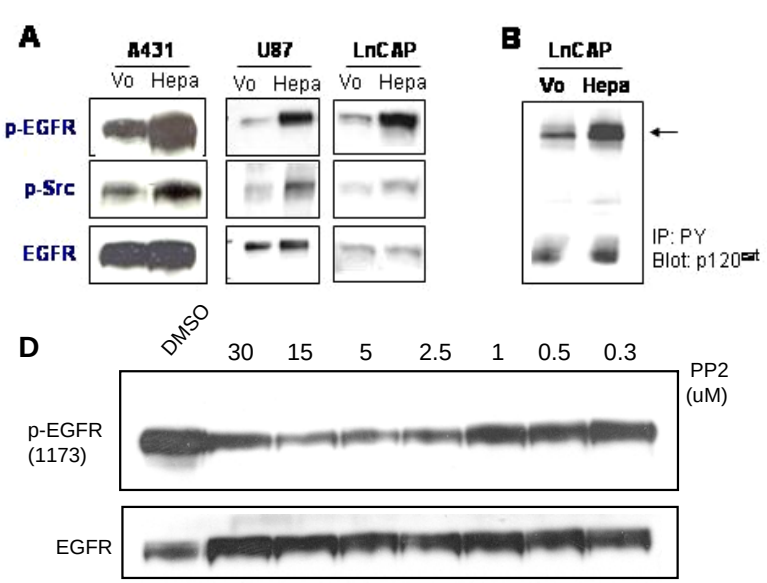

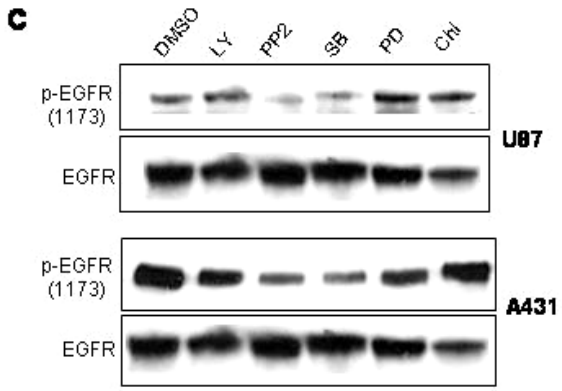

Figure 15. **Enhanced EGFR phosphorylation upon heparanase over expression is Src-dependent**. **A**. Src activation. Control, Vo, and heparanase transfected A431 (left), U87 (middle) and LnCAP (right) cell lysates were immunoblotted with anti-phospho-EGFR (upper panel), anti-phospho-Src (second panels) and anti-EGFR (bottom panels) antibodies. **B**. p120cat phosphorylation. Control, Vo, and heparanase transfected LnCAP cell lysates were immunoprecipitated (IP) with anti-phosphotyrosine (PY) antibody, followed by immunoblotting with anti-p120cat antibodies. **C**. Inhibitors screen. Heparanase transfected U87 (upper two panels) and A431 (lower two panels) were incubated (18 h, 37oC) with control vehicle (DMSO), PI 3-kinase (LY-294002), Src (PP2), p38 (SB 203580), and MAPK (PD 98059) inhibitors, or with chloroquine (Chl), which inhibits heparanase processing. Cell lysates were immunoblotted with anti-phospho-EGFR (first and third panels) and with anti-EGFR (second and fourth panels). **D**. Heparanase transfected A431 cells were incubated (18 h, 37oC) with control vehicle (DMSO), or with the indicated concentrations (μM) of the Src inhibitor PP2 and total cell lysates were immunoblotted with anti-phospho-EGFR (upper panel) and anti-EGFR (lower panel) antibodies.

Figure 16. Inhibition of experimental metastasis (A) and heparanase enzymatic activity (B) by N-acetylated and glycol split heparin

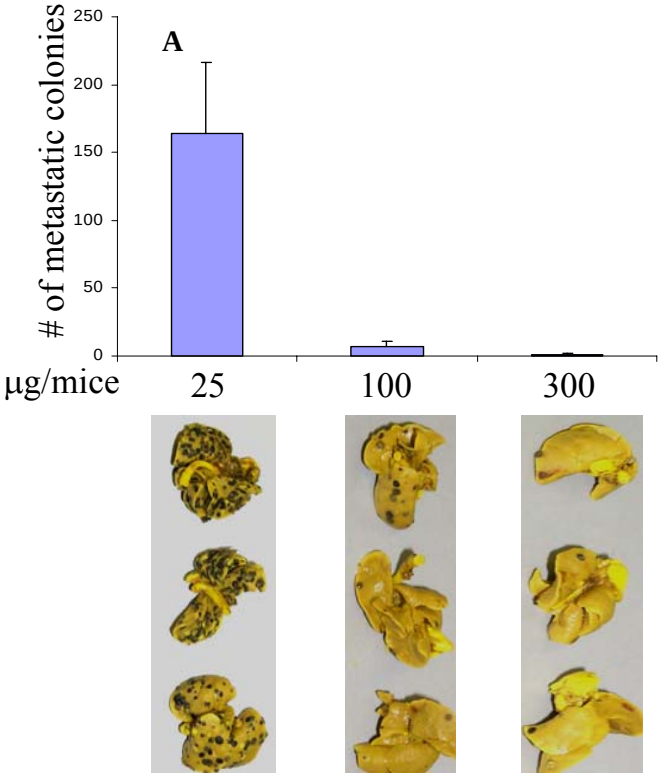

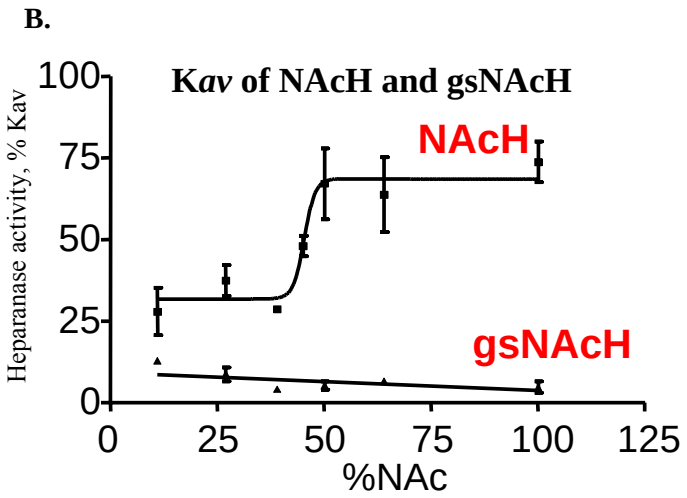

NAcH: N-acetylated heparin
gsNAcH: glycol-split N-acetylated heparin; note complete inhibition of heparanase activity in the presence of gsNAcH

Figure 17 ***In vivo*** **administration of anti-heparanase si-RNA inhibits primary DU145 tumor growth**

Percentage of tumor-bearing mice **before** & **after** the treatment

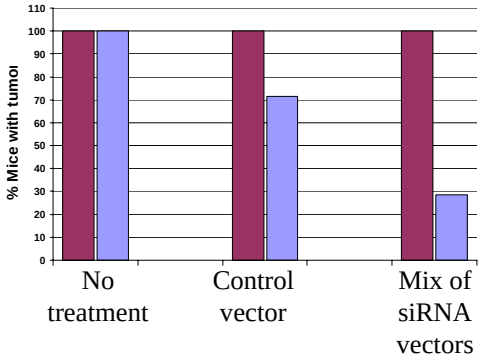

Weight of tumors after treatment

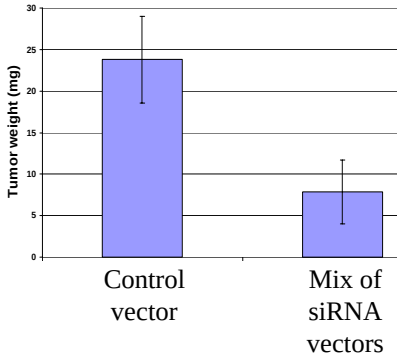

Macroscopic appearance of the DU145 tumors in mice treated with:

1. control vector 2. mix of siRNA vectors

Figure 18. Heparanase immunodetection in DU145 tumors electroporated with Vo (left), untreated (middle) and electroportaed with pSH and pSi vector mixture (right). Tumor tissue harvested on day 28 of the experiment was processed for immunohisto chemical analysis of HPSE expression (reddish staining). Original magnification, X 200. Note the extensive staining in tumors untreated or electroporated with empty pSUPER vector versus the weak or no staining in pSH/pSi-treated tumors.

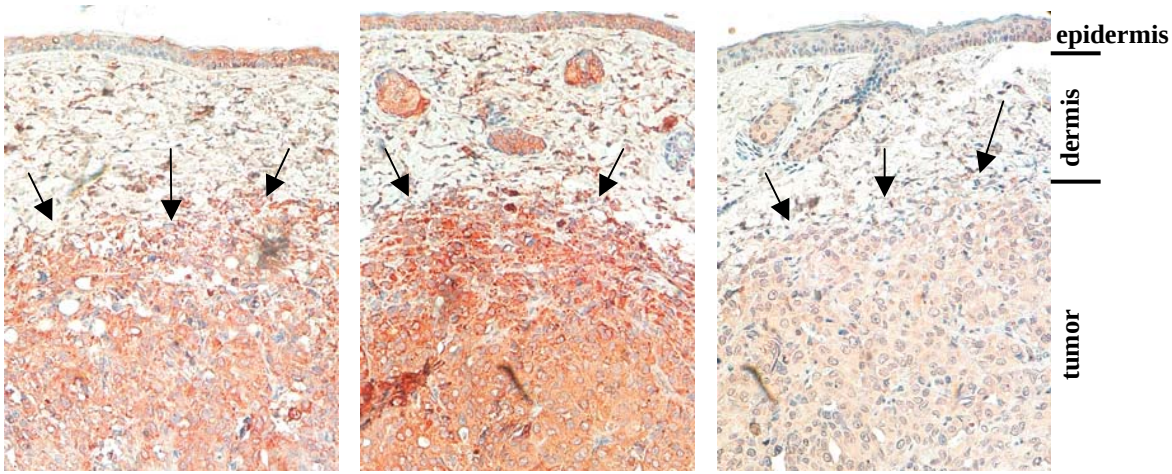

Figure 19. Effective and specific action of anti-human heparanase siRNA in DU145 cells

RT-PCR

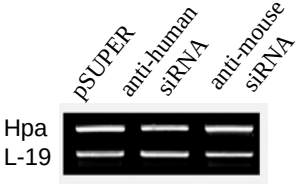

Heparanase activity

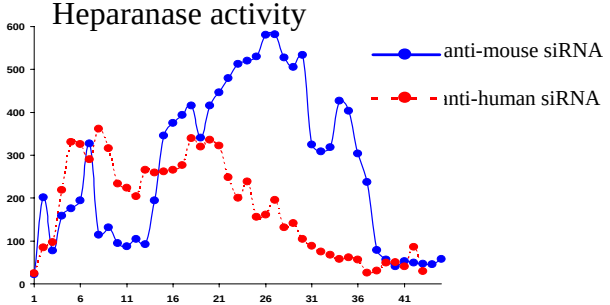

Oncogene (2006) 25, 3939–3947

www.nature.com/onc

ORIGINAL ARTICLE

Tumor suppressor p53 regulates heparanase gene expression

L Baraz[1], Y Haupt[2], M Elkin[1], T Peretz[1] and I Vlodavsky[3]

[1]*Department of Oncology, Hadassah-University Medical Center, Jerusalem, Israel;* [2]*Lautenberg Center for General and Tumor Immunology, The Hebrew University Hadassah Medical School, Jerusalem, Israel and* [3]*Cancer and Vascular Biology Research Center, The Bruce Rappaport Faculty of Medicine, Technion, Haifa, Israel*

Mammalian heparanase degrades heparan sulfate, the most prominent polysaccharide of the extracellular matrix. Causal involvement of heparanase in tumor progression is well documented. Little is known, however, about mechanisms that regulate heparanase gene expression. Mutational inactivation of tumor suppressor p53 is the most frequent genetic alteration in human tumors. p53 is a transcription factor that regulates a wide variety of cellular promoters. In this study, we demonstrate that wild-type (wt) p53 binds to heparanase promoter and inhibits its activity, whereas mutant p53 variants failed to exert an inhibitory effect. Moreover, p53-H175R mutant even activated heparanase promoter activity. Elimination or inhibition of p53 in several cell types resulted in a significant increase in heparanase gene expression and enzymatic activity. Trichostatin A abolished the inhibitory effect of wt p53, suggesting the involvement of histone deacetylation in negative regulation of the heparanase promoter. Altogether, our results indicate that the heparanase gene is regulated by p53 under normal conditions, while mutational inactivation of p53 during cancer development leads to induction of heparanase expression, providing a possible explanation for the frequent increase of heparanase levels observed in the course of tumorigenesis.
Oncogene (2006) **25,** 3939–3947. doi:10.1038/sj.onc.1209425; published online 13 February 2006

Keywords: heparanase; p53; gene expression; promoter activity

Introduction

Heparanase (endo-β-D-glucuronidase) degrades heparan sulfate (HS), the main polysaccharide component of the extracellular matrix (ECM) (Hulett *et al*., 1999; Kussie *et al*., 1999; Toyoshima and Nakajima, 1999; Vlodavsky *et al*., 1999). Heparan sulfate plays a key role in the self-assembly and integrity of the ECM (Timpl, 1996; Bernfield *et al*., 1999; Kalluri, 2003). Malignant tumor growth, neovascularization, and metastasis represent invasive processes that involve enzymatic disintegration of the ECM. Heparanase cleavage of HS in the ECM, particularly in epithelial and subendothelial basement membranes, is, therefore, a critical determinant in cancer development and progression (Hulett *et al*., 1999; Kussie *et al*., 1999; Toyoshima & Nakajima, 1999; Friedmann *et al*., 2000; El-Assal *et al*., 2001; Gohji *et al*., 2001; Koliopanos *et al*., 2001; Rohloff *et al*., 2002). Heparanase is preferentially expressed in human tumors (Kosir *et al*., 1999; Vlodavsky *et al*., 1999; Zcharia *et al*., 2001) in correlation with metastatic potential, tumor vascularity and reduced postoperative survival of cancer patients (Kosir *et al*., 1999; Friedmann *et al*., 2000; El-Assal *et al*., 2001; Gohji *et al*., 2001; Koliopanos *et al*., 2001; Zcharia *et al*., 2001; Rohloff *et al*., 2002).

Expression of human heparanase in normal cells is restricted primarily to cytotrophoblasts, keratinocytes and activated cells of the immune system (Vlodavsky *et al*., 1999), suggesting that in most cell types, heparanase promoter is subjected to a constitutive inhibitory control. Given the potential tissue damage that could result from uncontrolled cleavage of HS, tight regulation of heparanase gene expression is essential. In previous studies, several transcription factors (i.e. SP1 and ETS (Jiang *et al*., 2002; Lu *et al*., 2003), estrogen (Elkin *et al*., 2003), glucose (Maxhimer *et al*., 2005) and alterations in the promoter methylation levels (Shteper *et al*., 2003; Ogishima *et al*., 2005a, b) were implicated in the regulation of heparanase transcription. However, the precise molecular mechanisms responsible for heparanase overexpression in a wide variety of cancer types remain unknown.

The process of carcinogenesis involves gain of oncogene activity and loss of tumor suppressor gene function. A key tumor suppressor gene that is often lost upon transformation is p53 (Vogelstein *et al*., 2000; Vousden and Lu, 2002). Wild-type (wt) p53 is a transcription factor that limits aberrant cell growth in response to various stress conditions, such as DNA damage, oncogene activation, hypoxia and the loss of normal cell contacts (Sionov and Haupt, 1999; Haupt and Haupt, 2004). Wild type, but not mutant p53, binds to a specific consensus DNA sequence in the promoter region of target genes and transactivates their expression

Correspondence: Professor I Vlodavsky, Cancer and Vascular Biology Research Center, The Bruce Rappaport Faculty of Medicine, Technion, Haifa 31096, Israel.
E-mail: vlodavsk@cc.huji.ac.il
Received 15 August 2005; revised 5 December 2005; accepted 30 December 2005; published online 13 February 2006

(el-Deiry *et al*., 1992, 1993; Okamoto and Beach, 1994; Miyashita and Reed, 1995). On the other hand, some promoters are negatively regulated by wt p53. These include MMP-1 (Sun *et al*., 1999), alpha-fetoprotein (Lee *et al*., 1999), PSA (Gurova *et al*., 2002), and Cox-2 (Subbaramaiah *et al*., 1999). Apart of the growth inhibitory function of wt p53, the loss of other functions of p53 can contribute to tumorigenesis, as well. Of much importance is the identification of 'novel' p53 effectors that mediate such functions. Since heparanase is overexpressed in a wide variety of malignancies where p53 is mutated, we hypothesized that p53 may regulate heparanase gene expression. Our results show that wt p53 inhibits transcription of the heparanase gene by direct binding to its promoter. This inhibition involves recruitment of histone deacetylases (HDACs). In contrast, two tumor-derived p53 mutants have lost this repression activity. Together, these findings provide evidence that an important target of p53 mediated gene repression is heparanase. Thus, along with its well-documented effects on cell proliferation, an important outcome of p53 loss is elevation of heparanase gene expression that promotes tumorigenesis, affecting pathologic tumor-stromal interactions (i.e. ECM degradation, metastasis, angiogenesis). In addition, transcriptional activation of heparanase may represent a new molecular mechanism through which mutated p53 promotes tumorigenesis. Interestingly, a p53 mutant, p53H175R, was found to elevate heparanase expression, identifying heparanase as a new transcriptional target for this and possibly other p53 mutants.

Results

Elimination or inhibition of wt p53 increases heparanase gene expression and enzymatic activity

To test whether p53 regulates heparanase gene expression, we first compared the levels of endogenous heparanase (hpa) expression in mouse embryonic fibroblasts (MEF) derived from wt or p53 knockout ($p53^{-/-}$) mice, applying semiquantitative reverse transcription polymerase chain reaction (RT–PCR). Heparanase levels were elevated in $p53^{-/-}$ MEF and undetectable in the wt counterparts (Figure 1a, top). Heparanase enzymatic activity was also significantly higher in $p53^{-/-}$ than in wt MEF lysates (Figure 1a, bottom).

To rule out the possibility that the two MEF lines acquired additional genetic alterations that can affect heparanase regulation, p53 gene silencing approach was applied using small interfering RNA directed against p53 (p53siRNA). For this purpose, we used human embryonic lung fibroblasts, WI-38, immortalized by the introduction of a human telomerase gene (hTERT) (Milyavsky *et al*., 2003). WI-38/hTERT cells were transduced with lentivirus containing p53siRNA, or with lentivirus alone and tested for heparanase expression after 72 h. As demonstrated in Figure 1b, downregulation of p53 resulted in increased heparanase mRNA expression (Figure 1b, top), as well as heparanase enzymatic activity (Figure 1b, bottom).

Next, we measured the effect of p53 protein inhibition on heparanase mRNA transcription in WI-38/hTERT cells. p53 activity was downregulated by expression of the genetic suppressor element 56 (GSE-56), which corresponds to the C-terminal portion of p53 and whose expression results in accumulation of p53 in its inactive conformation and in inhibition of p53 activity (Ossovskaya *et al*., 1996). Expression of GSE56 in WI-38/hTERT cells resulted in a pronounced increase of both heparanase mRNA expression (Figure 1c, top) and enzymatic activity (Figure 1c, bottom). These results support the notion that wt p53 suppresses heparanase gene expression and consequently leads to an overall reduction in heparanase enzymatic activity.

Heparanase is upregulated in H1299 cells expressing a temperature sensitive (ts) p53 mutant

In order to further investigate the inhibitory effect of p53 on heparanase promoter activity, we used p53-negative H1299 lung adenocarcinoma cells, stably transfected with a temperature sensitive (ts) Val_{135} mutant form of p53. This mutant protein contains a substitution from cysteine to valine at position 135, and possesses wt activity at 32°C, but a mutant inactive conformation at 37°C (Michalovitz *et al*., 1990). H1299Val_{135} cells were transfected with a reporter construct containing luciferase gene driven by the heparanase promoter (*HPSE*-LUC) (Elkin *et al*., 2003; Zcharia *et al*., 2005), or with *p21*-LUC plasmid in which LUC expression is driven by the p21 promoter, one of the main targets of p53. Figure 2a demonstrates a markedly reduced heparanase promoter activity in lysates of H1299Val_{135} cells cultured at 32°C compared with lysates derived from cells grown at 37°C. In contrast, the *p21* promoter was induced at 32°C, due to wt p53 activity. In the parental p53-negative H1299 cells the activity of both *HPSE* and *p21* promoters was unchanged by the temperature shift (not shown), indicating that the observed differences in promoter activities were due to inactivation of ts p53 rather than to a general effect of the temperature change on gene expression. Enzymatic activity of heparanase (Figure 2b) was much higher in lysates of H1299Val_{135} cells maintained at 37°C and therefore bearing the inactive form of p53, than in lysates prepared from cells cultured at 32°C when p53 acquires a wt phenotype. Heparanase activity determined in non-transfected H1299 cells incubated at 32°C was similar to that of cells maintained at 37°C (not shown).

Heparanase promoter activity is repressed by wt, but not mutant p53

To analyse the effect of p53 on heparanase promoter activity, we introduced *HPSE*-LUC plasmid into p53-negative human osteosarcoma SaoS-2 cells. Along with *HPSE*-LUC, the cells were co-transfected with a plasmid expressing either wt p53, or one of its three

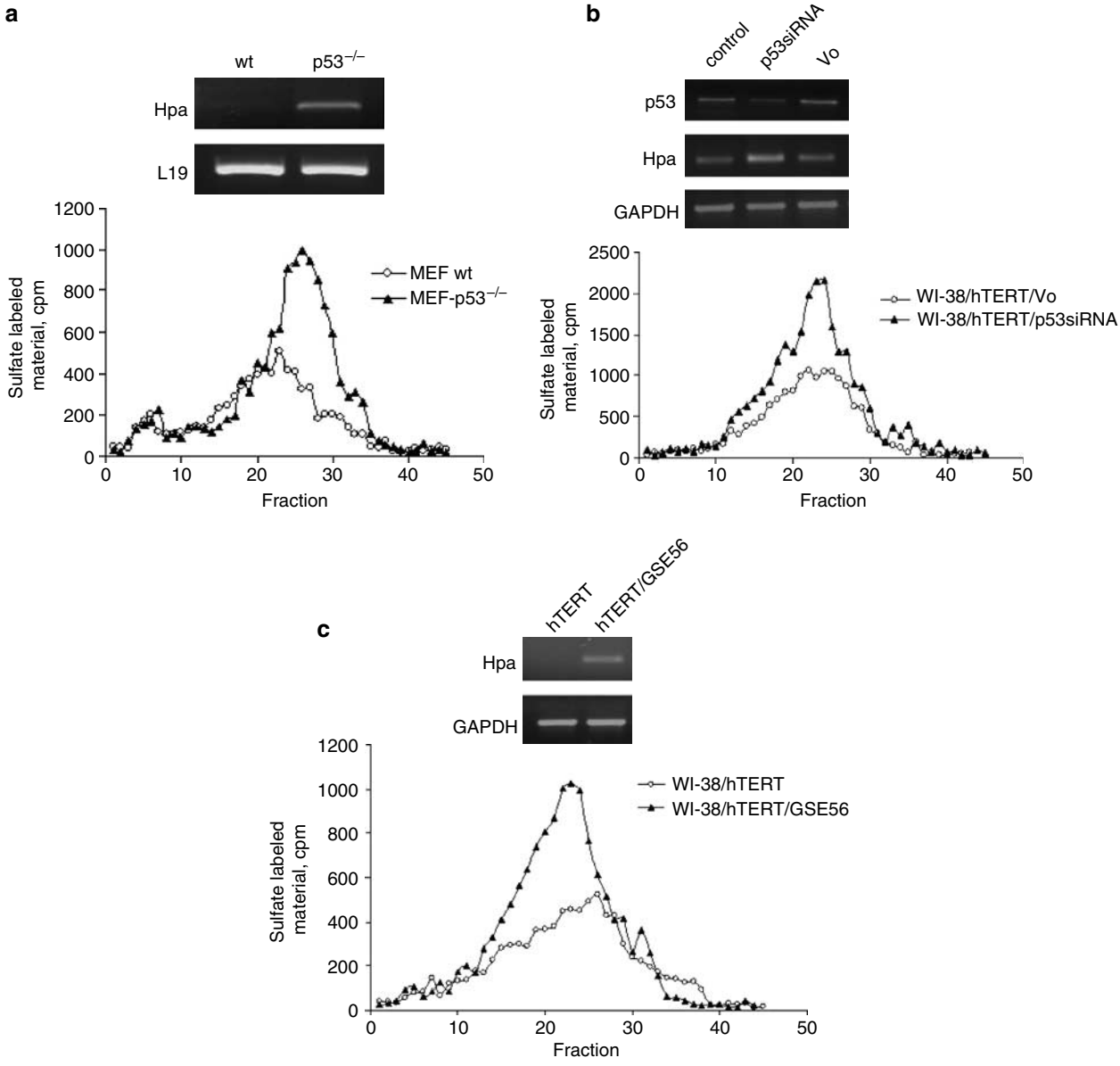

Figure 1 Effect of wt p53 elimination or inhibition on heparanase expression and enzymatic activity. (**a**) Increased heparanase expression in $p53^{-/-}$ knock-out mouse embryonic fibroblasts (MEF). Top: Heparanase (Hpa) mRNA expression. RNA isolated from wt and p53 knock-out ($p53^{-/-}$) MEF was reverse transcribed to cDNA and subjected to comparative semiquantitative PCR, as described in 'Materials and methods'. Aliquots (10 μl) of the PCR products were separated by 1.5% agarose gel electrophoresis and visualized. Bottom: Enzymatic activity. MEF lysates (1×10^6 cells) obtained from wt (○) or $p53^{-/-}$ (▲) mice were normalized for equal amounts of protein and incubated (18 h, 37°C, pH 5.8) with sulfate labeled ECM. Labeled degradation fragments released into the incubation medium were analysed by gel filtration over Sepharose CL-6B column, as described in 'Materials and methods'. Sulfate-labeled material eluted in fractions 15–35 is composed of heparan sulfate degradation fragments. (**b**) siRNA-mediated silencing of p53 elevates heparanase expression. WI-38/hTERT cells were infected with lentiviral vector encoding for p53siRNA or control vector (Vo). Top: Heparanase (Hpa) mRNA expression. RNA was isolated 72 h postinfection, reverse transcribed to cDNA and subjected to comparative semiquantitative PCR. The number of cycles for heparanase was 36 since its expression in these cells is very low. Bottom: Enzymatic activity. WI-38/hTERT cells (1×10^6), infected with either lentiviral vector containing p53siRNA (▲) or control vector (○) were lysed 3 days postinfection, normalized for equal protein, and cell lysates were tested for heparanase enzymatic activity. (**c**) Functional inactivation of p53 enhances heparanase expression. Top: Heparanase (Hpa) mRNA expression. RNA was isolated from WI-38 cells stably transfected with telomerase gene hTERT alone (WI-38/hTERT), or with hTERT plus the dominant negative form of p53 (WI-38/hTERT/GSE56). Bottom: Enzymatic activity. Cell lysates of 0.5×10^6 WI-38/hTERT (○) or WI-38/hTERT/GSE56 (▲) cells were normalized for equal protein and tested for heparanase enzymatic activity.

mutant variants (p53-V173L, p53-R175 H, p53-H179Q), commonly found in human cancer. Expression of wt p53 in SaoS-2 cells led to a marked decrease in heparanase promoter activity measured by the luciferase assay, reaching up to a ~9-fold reduction (Figure 3a). In contrast, none of the three tested p53 mutants displayed

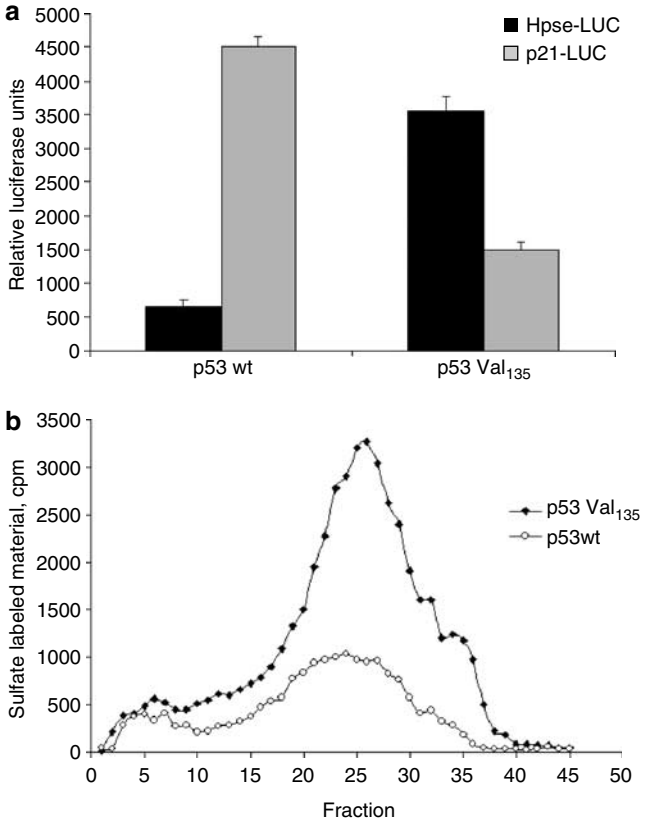

Figure 2 Temperature-induced inactivation of p53 C135 V variant results in decreased heparanase promoter and enzymatic activities. (**a**) Promoter activity. H1299Val$_{135}$ cells were transiently transfected with LUC reporter gene driven by either heparanase (*HPSE*-LUC) or p21 (*p21*-LUC) promoters. Immediately after transfection, the cells were incubated at 32°C or 37°C for 48 h, lysed and measured for luciferase activity. The relative light units (±s.d.) in each sample were normalized against beta-galactosidase activity, measured by a colorimetric assay. (**b**) Heparanase activity. Lysates of 1×10^6 p53 wt (○) or p53 Val$_{135}$ (◆) cells were analysed for heparanase activity as described in 'Materials and methods'.

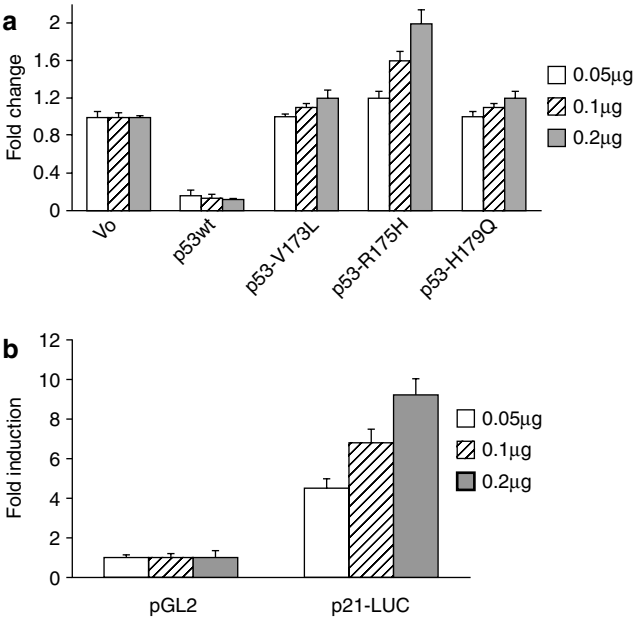

Figure 3 Effect of p53 on heparanase promoter activity. (**a**) Dose-dependent repression of heparanase promoter activity by wt, but not mutant p53. SaoS-2 cells were co-transfected with 0.05 µg luciferase reporter gene driven by the heparanase promoter (*HPSE*-LUC) and with increasing amounts (0.05, 0.1 and 0.2 µg/well) of empty vector (Vo), or vectors encoding for wt or one of the three mutated variants (p53-V173L, p53-R175 H and p53-H179Q) of p53. Steady amount of DNA in each well was kept by addition of pcDNA3 vector with no insert. Luciferase light units and beta-galactosidase colorimetric assay activities were measured 24 h later. The graph represents fold difference ±s.d., as compared to the Vo control (SaoS-2 cells transfected with empty pcDNA3 vector only). Three independent experiments were performed in quadruplicates. (**b**) Wt p53 does not affect SV40 promoter activity in pGL2 and activates the p21 promoter (*p21*-LUC). Experiment was performed as in A, except that pGL2 or *p21*-LUC plasmids, instead of *HPSE*-LUC, were co-expressed with increasing amounts of wt p53 protein.

any repression ability (Figure 3a). Interestingly, expression of p53-R175 H, which is a 'hot spot' mutant in human cancer (Vousden and Lu, 2002) caused a moderate (up to 2-fold) but consistently reproducible activation of heparanase promoter at the highest amount of the plasmid (Figure 3a). The *p21*-LUC plasmid was used as a marker for wt p53 functionality. As expected, LUC expression was elevated in a dose-dependent manner as a result of co-transfection with increasing amounts of the wt p53 plasmid (Figure 3b). Under the same conditions, expression of luciferase driven by the SV40 promoter (pGL2-control vector) was not altered by co-transfection with increasing amounts of wt p53, demonstrating that the effect of p53 on heparanase promoter activity was not the result of a general inhibition of transcription (Figure 3b). These results indicate that unlike wt p53, p53 mutants do not repress the heparanase promoter. Moreover, certain mutants (e.g. p53R175 H) may activate the heparanase promoter.

Wild-type p53 binds the heparanase promoter

In order to demonstrate direct binding of the p53 protein to regulatory sequences of the heparanase gene, we performed chromatin immunoprecipitation (ChIP) assay with DNA isolated from WI-38/hTERT and WI-38/hTERT/GSE56 cells. DNA was sonicated into fragments of an average size of 500 bp. We used five sets of primers (HPSEp-1-5) designed to amplify ~200 bp PCR products, distributed over the entire length of the heparanase promoter (as indicated in 'Materials and methods'). We looked for the promoter sequences in nuclear extracts of WI-38/hTERT vs WI-38/hTERT/GSE56 cells, immunoprecipitated with antibody against p53. As demonstrated in Figure 4, a sequence of the heparanase (HPSE) promoter region amplified by primer set HPSEp-4 (located at position 2409–2687 relative to the origin of the promoter), but not by the other primer sets, was reproducibly present in the chromatin DNA immunoprecipitated with anti-p53 antibody from WI-38/hTERT (lane1), but not WI-38/hTERT/GSE56 nuclear extracts (lane 2) (Figure 4, HPSEp-4). This experiment demonstrates direct binding

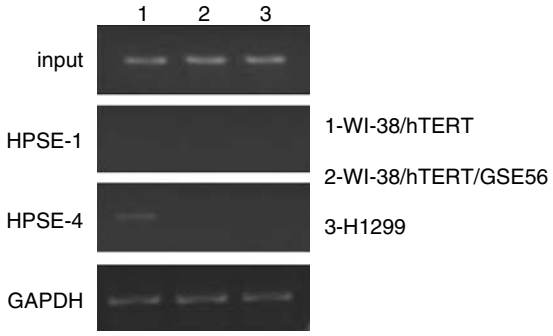

Figure 4 p53 protein binds to heparanase promoter. Chromatin immunoprecipitation (ChIP) analysis was performed for WI-38/hTERT (wt p53), WI-38/hTERT/GSE56 (inactivated p53), or H1299 (p53-negative) cells to demonstrate p53 binding to each of the heparanase promoter sites. Following crosslinking of proteins to DNA, DNA was fragmented, and the p53 protein was immunoprecipitated with specific antibody. PCR analysis was performed on the immunoprecipitated DNA samples using heparanase-specific primers, as described in 'Materials and methods'.

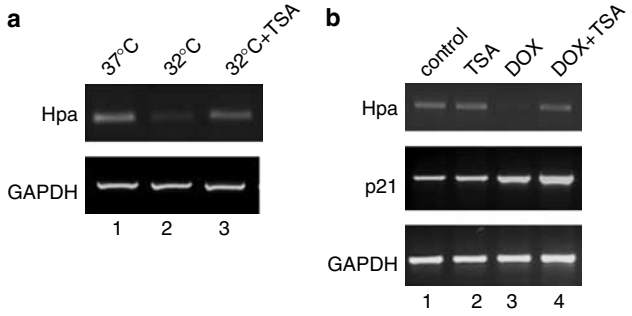

Figure 5 Transcriptional repression of heparanase by p53 is inhibited by the HDAC inhibitor TSA. (**a**) H1299Val$_{135}$ cells. RT–PCR analysis of heparanase mRNA levels in H1299Val$_{135}$ cells at 37°C (lane 1, mutant p53) and following temperature shift to 32°C for 24 h (wt p53 activity) in the absence (lane 2) or presence (lane 3) of 100 nM TSA (Sigma, St Louis, Missouri, USA). The decrease in heparanase (Hpa) mRNA due to the temperature shift and induction of p53 is largely reversed by incubation with TSA. In contrast, the level of the housekeeping gene GAPDH is not affected by the temperature shift or TSA treatment. (**b**) MCF-7 cells. RT–PCR analysis of heparanase levels in MCF-7 cells treated for 6 h with 1 μg/ml DOX (Sigma, St Louis, Missouri, USA), an inducer of p53, indicates that DOX treatment leads to repression of heparanase gene expression (lane 3). TSA treatment alone had no effect on heparanase expression (lane 2). Repression of heparanase by DOX is abrogated by 100 nM TSA (lane 4). p21 expression level is induced as a result of DOX treatment and p53 activation (lanes 3 and 4), but is not affected by TSA treatment alone (lane 2).

of wt p53 to the heparanase promoter in proximity to the HPSEp-4 region. No PCR product was obtained from p53-null H1299 cell lysates precipitated with anti-p53 antibody (lane 3), confirming the specificity of the assay.

Trichostatin A inhibits p53-mediated repression of heparanase

Mechanisms of transcriptional repression by p53 are poorly understood; however, association between this activity of p53 and the recruitment of HDAC to the regulatory sequences of target genes has been observed (Murphy *et al*., 1999). We investigated whether trichostatin A (TSA), a potent and specific inhibitor of HDAC activity (Yoshida *et al*., 1990), is able to inhibit suppression of heparanase expression by p53. Initially, we used H1299Val$_{135}$ cells grown at 37°C or temperature-shifted to 32°C for 18 h in the presence or absence of 100 nM TSA. Induction of wt p53 following temperature shift to 32°C resulted in a significant reduction in heparanase mRNA, measured by RT–PCR. However, in the presence of TSA, this decrease was inhibited and heparanase expression levels remained unchanged. In contrast, GAPDH levels were not altered by the temperature shift or incubation with TSA (Figure 5a).

To extend this observation, human breast carcinoma cells (MCF-7) were analysed following activation of endogenous wt p53 protein by the DNA-damaging agent, doxorubicin (DOX) (el-Deiry *et al*., 1993). As demonstrated in Figure 5b, treatment of MCF-7 cells with DOX resulted in a pronounced decrease in heparanase mRNA level after 6 h. This reduction was abrogated by TSA treatment, while TSA alone had no detectable effect on heparanase mRNA level. As a marker for p53 activation, we used p21 whose expression was significantly elevated after DOX treatment (Figure 5b). These results demonstrate that DOX-induced activation of endogenous p53 leads to down-regulation of heparanase gene expression. TSA specifically inhibits the repression of heparanase following p53 activation. Thus, HDAC activity may be an integral component of the p53-mediated repression of the heparanase gene.

Discussion

Overexpression of heparanase in malignant tumors, as well as its potential contribution to cancer progression (i.e. enhanced primary tumor growth, invasiveness, angiogenesis), are well documented (Vlodavsky and Friedmann, 2001). However, despite extensive studies on upregulation of the heparanase gene during tumorigenesis, little is known about physiologically relevant repressors of heparanase gene transcription, responsible for the low or undetectable levels of heparanase under normal conditions. The present study demonstrates, for the first time, that the heparanase gene is a molecular target of p53-mediated transcriptional repression. We show that wt p53 is a powerful inhibitor of heparanase transcription. In cells lacking p53, heparanase expression is elevated, suggesting that the mere absence of p53 is sufficient to activate the heparanase promoter. Tumor-derived p53 mutants no longer exert this inhibitory ability. Interestingly, at least one of the six most common cancer-associated p53 mutants, p53-R175H, upregulates heparanase promoter activity. This effect, albeit moderate, may be attributed to a direct interaction between the p53-R175H mutant and the

heparanase promoter, via a mechanism similar to p53-R175H-mediated activation of the VEGF promoter (Weisz *et al*., 2004), or to indirect activation of heparanase via the transcription factor EGR-1. It has recently been demonstrated that expression of EGR-1, a known inducer of heparanase transcription (de Mestre *et al*., 2003; Ogishima *et al*., 2005a), is markedly upregulated by the p53-R175H protein (Weisz *et al*., 2004).

Our results implicate p53 in regulating heparanase expression not only in carcinoma cells *per se* but also in fibroblasts. A marked stimulation of heparanase gene expression and enzymatic activity has been demonstrated in MEF derived from $p53^{-/-}$ mice (Figure 1a). Moreover, transcriptional (siRNA) or functional (GSE 56) inactivation of p53 in telomerase-immortalized WI-38 human fibroblasts led to increased heparanase expression (Figure 1a and b). Recently, the critical importance in carcinogenesis of stromal elements (e.g. carcinoma-associated fibroblasts, CAFs) and their secreted factors, is increasingly documented (Bhowmick and Moses, 2005). Among other mechanisms, it was suggested that stromal cellular elements may contribute to the malignant potential of the tumor by producing heparanase (Friedmann *et al*., 2000; Marchetti *et al*., 2000). While normal fibroblasts lack detectable heparanase activity (Nadav *et al*., 2002, and our unpublished observations), elevated levels of the heparanase protein were detected in fibroblasts associated with deeply invading colon carcinoma (Friedmann *et al*., 2000). Recently, it has been shown that somatic p53 mutations are responsible for the tumor-supporting activities exerted by CAFs (Kiaris *et al*., 2005). Tumors containing p53-deficient stromal fibroblasts developed faster and were more aggressive than their counterparts with fibroblasts bearing wt p53 (Kiaris *et al*., 2005). Our results propose a molecular pathway through which CAFs, due to the loss of functional p53, may become an independent source of heparanase in the tumor vicinity, thus contributing to tumor progression.

As a transcriptional regulator, p53 can both induce and repress the expression of target genes (Vousden and Lu, 2002). While acting as an activator of transcription, p53 binds DNA directly in a sequence-specific manner through a highly conserved DNA-binding domain (el-Deiry *et al*., 1992). In contrast to the well-studied mechanisms of p53 activation, the exact nature of p53-mediated repression of target genes is not fully understood. Three mechanisms were proposed for p53-mediated transcriptional repression (Ho and Benchimol, 2003). The first two may occur in the absence of DNA binding and involve interference with either the function of DNA-binding transcriptional activators (Lee *et al*., 1999; Sun *et al*., 1999), or the basal transcriptional machinery (Seto *et al*., 1992; Farmer *et al*., 1996; Subbaramaiah *et al*., 1999). The third mechanism for p53-dependent transcriptional repression involves direct binding to the promoter region of a target gene and alteration of the chromatin structure within the promoter by recruiting HDAC (Murphy *et al*., 1999; Mirza *et al*., 2002; Ho and Benchimol, 2003). Recruitment of HDACs to the promoter of p53-repressed genes results in enzymatic deacetylation of histones on chromatin, creating a transcriptionally unfavourable environment (Zilfou *et al*., 2001; Allison and Milner, 2004). We found that wt p53 binds directly to the heparanase promoter. The HDAC inhibitor TSA completely abrogated the decrease in heparanase mRNA level observed in MCF-7 cells following DOX treatment. Similarly, the decrease in heparanase level following temperature switch in $H1299Val_{135}$ cells was reversed by TSA treatment (Figure 5). These results strongly suggest that negative regulation of heparanase gene expression by p53 involves HDAC recruitment.

In conclusion, we have demonstrated that the heparanase gene is under a strict negative control by wt tumor suppressor p53 and its expression is stimulated by the loss of wt p53 activity in cell culture. It is therefore conceivable that the heparanase gene is constitutively repressed by p53 *in vivo*. As a result of this negative control, combined with hypermethylation of the heparanase promoter region (Shteper *et al*., 2003; Ogishima *et al*., 2005a, b), normal cells remain heparanase-negative. In contrast, inactivation of negative regulators of heparanase gene transcription along with the stimulatory effect of activating factors such as EGR-1, may collectively contribute to the increased heparanase expression in human tumors. Our results provide the first evidence for a functional involvement of p53 in heparanase regulation under normal and pathological conditions, and may have implications in the treatment of tumors overexpressing heparanase and bearing mutations in p53.

Materials and methods

Cells

Human osteosarcoma SaoS-2, human breast carcinoma MCF-7, and human lung carcinoma H1299 cells, were obtained from the American Type Culture Collection (ATCC; Manassas, VA, USA). Human embryonic kidney 293T cells were kindly provided by Dr E Bacharach (Tel-Aviv University, Israel). Cells were maintained in Dulbecco's modified Eagle's medium (DMEM, 4.5 g glucose/l) or RPMI medium supplemented with 1 mM glutamine, 50 μg/ml streptomycin, 50 U/ml penicillin and 10% fetal calf serum (FCS) at 37°C in a 5% humidified incubator. Mouse embryonic fibroblasts were generated from wt or $p53^{-/-}$ mice and cultured in DMEM supplemented with 1 mM sodium pyruvate, 2 mM glutamine, 10 mM HEPES, 10 mM non-essential amino acids (Biological Industries, Beit Haemek, Israel). Cultures of bovine corneal endothelial cells were established from steer eyes and maintained in DMEM (1 g glucose/liter) supplemented with 5% newborn calf serum, 10% FCS and 1 ng/ml bFGF, as described (Vlodavsky *et al*., 1999). Confluent cell cultures were dissociated with 0.05% trypsin and 0.02% EDTA in phosphate-buffered saline (PBS) and sub-cultured at a split ratio of 1:8 (Vlodavsky *et al*., 1999). $H1299Val_{135}$ cells were generated by introducing the $p53Val_{135}$ expression plasmid into H1299 cells (a gift from Dr M Oren, The Weizmann Institute of Science, Rehovot, Israel). Cells were maintained at 37°C, a temperature at which p53 acquires a mutant conformation. To convert p53 into the wt conformation, cells were shifted to 32°C for at least 12 h.

Primary human embryonic lung fibroblasts (WI-38), stably expressing hTERT alone or hTERT and GSE56, were kindly provided by Dr V Rotter (The Weizmann Institute of Science, Rehovot, Israel). These cells were grown in MEM supplemented with 10% FCS, 1 mM sodium pyruvate, 2 mM L-glutamine, and antibiotics.

Preparation of sulfate labelled ECM
Bovine corneal endothelial cells were plated into 35-mm tissue culture dishes at an initial density of 2×10^5 cells/ml and cultured as described above, except that 4% dextran T-40 was included in the growth medium (Vlodavsky *et al*., 1999). On day 12, the subendothelial ECM was exposed by dissolving the cell layer with PBS containing 0.5% Triton X-100 and 20 mM NH_4OH, followed by four washes with PBS (Vlodavsky *et al*., 1999). The ECM remained intact, free of cellular debris and firmly attached to the entire area of the tissue culture dish. To produce sulfate labeled ECM, $Na_2^{35}SO_4$ (25 μCi/ml) (Amersham, Buckinghamshire, UK) was added on days 2 and 5 after seeding and the cultures were incubated with the label without medium change and processed as described (Vlodavsky *et al*., 1999). Nearly 80% of the ECM radioactivity was incorporated into HSPGs.

Heparanase activity
Cells ($0.5–1 \times 10^6$ cells/ml) were lysed by three cycles of freezing and thawing in phosphate citrate buffer, pH 6.0, and incubated (16 h, 37°C, pH 6.0) with ^{35}S-labeled ECM. The incubation medium was centrifuged and the supernatant containing sulfate labeled degradation fragments was analysed by gel filtration on a Sepharose CL-6B column (0.9×30 cm^2) (Vlodavsky *et al*., 1983, 1999). Fractions (0.2 ml) were eluted with PBS and their radioactivity counted in a β-scintillation counter. Degradation fragments of HS side chains were eluted from Sepharose 6B at $0.5 < K_{av} < 0.8$ (peak II, fractions 15–30). Nearly intact HSPGs were eluted just after the V_0 ($K_{av} < 0.2$, peak I) (Vlodavsky *et al*., 1983, 1999; Goldshmidt *et al*., 2001). We have previously demonstrated that labeled fragments eluted in fractions 15–35 are degradation products of HS, as they were (i) five- to six-fold smaller than intact HS side chains; (ii) resistant to further digestion with papain and chondroitinase ABC; and (iii) susceptible to deamination by nitrous acid (Vlodavsky *et al*., 1983). Each experiment was performed at least three times and the variation in elution positions (K_{av} values) did not exceed $\pm 15\%$.

Reporter construct transfection and luciferase (LUC) assay
The 1.9-kb human heparanase promoter region [*HPSE* ($-1791/+109$)-LUC] was subcloned upstream of the *LUC* gene in a pGL2 basic reporter plasmid (Promega, Madison, WI, USA) (Elkin *et al*., 2003; Zcharia *et al*., 2005). SaoS-2 cells were seeded into 24-well plates at a density of 50 000 cells/well. Transfections were performed using FuGENE 6 Transfection Reagent (Roche, Indianopolis, IN, USA), according to the standard protocol. Reporter construct (0.05 μg/well) was mixed with 0.05, 0.1 and 0.2 μg of wt or p53 mutant constructs (p53-V173L, p53-R175 H and p53H179Q) (kindly provided by Dr K Vousden, The Beatson Institute for Cancer Research UK, and Dr M Oren, The Weizmann Institute of Science, Rehovot, Israel). Constant amounts of DNA in each well were preserved by addition of pcDNA3 plasmid without insert. Cells were harvested 24 h afterward and assayed for LUC activity using the Luciferase Reporter Assay system (Promega, Madison, WI, USA). H1299Val$_{135}$ cells were transfected with *HPSE*-LUC or *p21*-LUC. The relative light units were determined in each sample with a luminometer (Lumat LB 9507, Berthold Technologies) and results were normalized against beta-galactosidase activity measured by a colorimetric assay. Data are presented as the means of quadruplicates $\pm$ s.d., and all experiments were repeated at least three times with similar results.

Production of lentivector
293T cells at 80% confluence were co-transfected with lentiviral construct, encoding for siRNAp53 (a kind gift from Dr R Agami, The Netherlands Cancer Institute, The Netherlands), or control lentiviral construct without siRNA, pCMVdR8.91 packaging and pMD2-VSV-G envelope plasmids (a kind gift from Dr D Trono, University of Geneva, Switzerland) using FuGENE6 (Roche, Indianopolis, IN, USA), according to the manufacturer's instructions. Virus-containing culture supernatants were harvested 48–72 h post-transfection and pooled together. The supernatants were cleared of cell debris by spinning at $10\,000 \times g$ for 10 min, prior to centrifugation for 45 min at $100\,000 \times g$ in a Beckman centrifuge (Ti-50.2 rotor). The pellets were resuspended in PBS and used for infection of cultured WI-38/hTERT cells by spinoculation, as previously described (O'Doherty *et al*., 2000). Briefly, the pellets of 1×10^6 cells were mixed with lentiviruses and centrifuged at 1200 r.p.m. for 2 h at 25°C. Unbound virus was removed and the cells were resuspended in growth medium and cultured at 37°C. RNA expression was analysed 72 h later.

RNA isolation, cDNA synthesis and RT–PCR
RNA was isolated with TRIzol (Molecular Research Center, Cincinnati, OH, USA), according to the manufacturer's instructions and was quantitated by UV absorption. Deoxythymidylic acid oligomer (oligo dT)-primed reverse transcription was performed using 1 μg of total RNA in a final volume of 20 μl, and the resulting cDNA was further diluted to 100 μl. Comparative semiquantitative PCR was performed as follows: glyceraldehyde-3-phosphate dehydrogenase (GAPDH) or a ribosomal gene L19 mRNAs were first amplified at low-cycle number (GAPDH primer sequences: sense, 5′-CCACCCAT GGCAAATTCCATGGCA-3′; antisense, 5′-CTAGACGGCA GGTCAGGTCCACC-3′; L-19 sense: 5′-ATGCCAACTCT CGTCAACAG-3′; L-19 antisense: 5′-GCGCTTTCGTG CTTCCTT-3′). The resulting 600-bp products for GAPDH and L-19 were visualized by electrophoresis and ethidium bromide staining, and quantitated using the Scion Image Program (Scion Corporation). If needed, cDNA dilutions were adjusted and GAPDH reverse-transcription PCR products were reamplified to obtain similar intensities for GAPDH signals with all the samples. The adjusted amounts of cDNA were used for PCR with primers designed to amplify a PCR product specific for human heparanase (sense: 5′-ACAGTTC TAATGCTCAGTTGCTC-3′; antisense: 5′-CTTCAGCATC TTAGCCGTCTTT-3′), p21 (sense: 5′-ATGTCAGAACCG GCTGGGGA-3′; antisense 5′-GCCGTTTTCGACCCTGA GAG-3′), or p53 (sense: 5′-GTCGACCCCCCTCTGAGTC AGG-3′; antisense: 5′-GCTGGTGCAGGGGCCACGCG-3′). Only RNA samples that gave completely negative results in PCR without reverse transcriptase were further analysed. Intensity of each band was quantitated using Scion Image software. The PCR conditions were an initial denaturation at 95°C for 2 min, denaturation at 96°C for 15 s, annealing for 1 min at 58°C, and extension for 1 min at 72°C (28–33 cycles). Aliquots (10 μl) of the amplified cDNA were separated by 1.5% agarose gel electophoresis and visualized by ethidium bromide staining.

Chromatin immunoprecipitation (ChIP) assay

Human WI-38/hTERT and WI-38/hTERT/GSE56 cells were grown to 80% confluence. Formaldehyde (Merck, Darmstadt, Germany) was added directly into the culture medium to a final concentration of 1%. Fixation proceeded at room temperature for 10 min and was stopped by addition of glycine to a final concentration of 0.125 mol/l. Plates were rinsed twice with PBS, the cells were removed by scraping, and collected by centrifugation. Pellets were incubated with lysis buffer 1 (50 mM HEPES–KOH (pH 7.5), 140 mM NaCl, 1 mM EDTA, 10% glycerol, 0.5% NP-40, 0.25% Triton X-100 and protease inhibitors mixture), rocked at 4°C for 10 min and centrifuged. The pellets were then resuspended in lysis buffer 2 (200 mM NaCl, 1 mM EDTA, 0.5 mM EGTA, 10 mM TrisHCl, pH 8.0), rotated for 10 min at room temperature and collected by centrifugation. Pellets were resuspended in lysis buffer 3 (1 mM EDTA, 0.5 mM EGTA, 10 mM Tris HCl, pH 8.0, 0.1% deoxycholic acid), and sonicated into chromatin fragments of an average length of 500 bp, as determined empirically by agarose gel electrophoresis of fragmented chromatin samples. Chromatin was kept at −80°C. Chromatin solution was incubated with p53 specific antibody (FL393, Santa Cruz Biotechnology, Santa Cruz, CA, USA) at 4°C overnight with rotation. Immunoprecipitates were washed eight times with wash buffer (50 mM HEPES pH 7.6, 1 mM EDTA, 0.7% deoxycholic acid, 1% NP-40, 0.5 M LiCl, and protease inhibitors mixture). Elution of immune complexes was carried out by addition of 50 μl of elution buffer (50 mM TrisHCl, pH 8, 10 mM EDTA, 1% SDS) at 65°C for 15 min with brief vortexing every 2 min. Reverse crosslink was carried out by incubating at 65°C overnight. RNA and unbound proteins were removed by addition of 0.2 mg/ml of RNase A for 1 h at 37°C, followed by addition of 0.2 mg/ml of proteinase K for 2 h at 55°C. DNA was extracted by PCR Purification Kit (Genomed, Löhne, Germany). Recovered chromatin was suspended in 50 μl of TE, and PCR analysis performed using 5 μl of immunoprecipitated chromatin or input chromatin, using Titanium *Taq* PCR kit (BD Biosciences Clontech, Palo Alto, CA, USA). Amplifications (30 cycles) were performed using the following specific primers, yielding PCR products ~200 bp in length (location of primers relatively to the origin of the promoter is indicated in parentheses after each primer pair).

HPSEp-1 sense:	5′-GAAGCATAAGTGGGTGGATCTC-3′
HPSEp-1 antisense:	5′-GTCACCCAGGTTGGAATACAGT-3′ (57–277)
HPSEp-2 sense:	5′-CATGTAGACCACAAGGATGCAC-3′
HPSEp-2 antisense:	5′-GATTTCACCATGTCTGTCAGGA-3′ (970–1167)
HPSEp-3 sense:	5′-TTTTTGTAGAGATGGGGCTTCA-3′
HPSEp-3 antisense:	5′-TGTACCACCAATAAGGCAACAA-3′ (1815–2030)
HPSEp-4 sense:	5′-TTCACATCCCGATTCTGACA-3′
HPSEp-4 antisense:	5′-TTGCCAAATTTCTCCTCTGC-3′ (2409–2687)
HPSEp-5 sense:	5′-GAGGAAGGGATGAATACTCCA-3′
HPSEp-5 antisense:	5′-CTACTTCCTTGCTCGCTTTCC-3′ (2975–3274)

PCR products were separated by 1.5% agarose electrophoresis in Tris-borate-EDTA buffer and stained with ethidium bromide.

Acknowledgements

We thank Mrs Irit Cohen (Hadassah-University Medical Center, Jerusalem) for help with the ChIP assay, Professors Moshe Oren (Weizmann Institute of Science, Israel), Karen Vousden (Beaston Institute, UK), D Trono, (University of Geneva, Switzerland) and Reuven Agami (The Netherland Cancer Institute) for plasmids. This study was supported by a Postdoctoral Fellowship from the Israel Cancer Research Fund, by a Scholarship from the Women's Group of the Mexican Friends of the Hebrew University (awarded to LB) and by grants from the US Army (Award #W81XWH-04-1-0235), the Israel Science Foundation (Grant 532/02), the Israel Cancer Association, the Prostate Cancer Foundation, and by United States Public Service Grant RO1 CA 106456 from NCI, National Institutes of Health.

References

Allison SJ, Milner J. (2004). *Carcinogenesis* **25**: 1551–1557.
Bernfield M, Gotte M, Park PW, Reizes O, Fitzgerald ML, Lincecum J *et al*. (1999). *Annu Rev Biochem* **68**: 729–777.
Bhowmick NA, Moses HL. (2005). *Curr Opin Genet Dev* **15**: 97–101.
de Mestre AM, Khachigian LM, Santiago FS, Staykova MA, Hulett MD. (2003). *J Biol Chem* **278**: 50377–50385.
El-Assal ON, Yamanoi A, Ono T, Kohno H, Nagasue N. (2001). *Clin Cancer Res* **7**: 1299–1305.
el-Deiry WS, Kern SE, Pietenpol JA, Kinzler KW, Vogelstein B. (1992). *Nat Genet* **1**: 45–49.
el-Deiry WS, Tokino T, Velculescu VE, Levy DB, Parsons R, Trent JM *et al*. (1993). *Cell* **75**: 817–825.
Elkin M, Cohen I, Zcharia E, Orgel A, Guatta-Rangini Z, Peretz T *et al*. (2003). *Cancer Res* **63**: 8821–8826.
Farmer G, Colgan J, Nakatani Y, Manley JL, Prives C. (1996). *Mol Cell Biol* **16**: 4295–4304.
Friedmann Y, Vlodavsky I, Aingorn H, Aviv A, Peretz T, Pecker I *et al*. (2000). *Am J Pathol* **157**: 1167–1175.
Gohji K, Hirano H, Okamoto M, Kitazawa S, Toyoshima M, Dong J *et al*. (2001). *Int J Cancer* **95**: 295–301.
Goldshmidt O, Zcharia E, Aingorn H, Guatta-Rangini Z, Atzmon R, Michal I *et al*. (2001). *J Biol Chem* **276**: 29178–29187.
Gurova KV, Roklin OW, Krivokrysenko VI, Chumakov PM, Cohen MB, Feinstein E *et al*. (2002). *Oncogene* **21**: 153–157.
Haupt S, Haupt Y. (2004). *Cell Cycle* **3**: 912–916.
Ho J, Benchimol S. (2003). *Cell Death Differ* **10**: 404–408.
Hulett MD, Freeman C, Hamdorf BJ, Baker RT, Harris MJ, Parish CR. (1999). *Nat Med* **5**: 803–809.
Jiang P, Kumar A, Parrillo JE, Dempsey LA, Platt JL, Prinz RA *et al*. (2002). *J Biol Chem* **277**: 8989–8998.
Kalluri R. (2003). *Nat Rev Cancer* **3**: 422–433.
Kiaris H, Chatzistamou I, Trimis G, Frangou-Plemmenou M, Pafiti-Kondi A, Kalofoutis A. (2005). *Cancer Res* **65**: 1627–1630.
Koliopanos A, Friess H, Kleeff J, Shi X, Liao Q, Pecker I *et al*. (2001). *Cancer Res* **61**: 4655–4659.
Kosir MA, Wang W, Zukowski KL, Tromp G, Barber J. (1999). *J Surg Res* **81**: 42–47.
Kussie PH, Hulmes JD, Ludwig DL, Patel S, Navarro EC, Seddon AP *et al*. (1999). *Biochem Biophys Res Commun* **261**: 183–187.

Lee KC, Crowe AJ, Barton MC. (1999). *Mol Cell Biol* **19**: 1279–1288.
Lu WC, Liu YN, Kang BB, Chen JH. (2003). *Oncogene* **22**: 919–923.
Marchetti D, Li J, Shen R. (2000). *Cancer Res* **60**: 4767–4770.
Maxhimer JB, Somenek M, Rao G, Pesce CE, Baldwin Jr D, Gattuso P *et al*. (2005). *Diabetes* **54**: 2172–2178.
Michalovitz D, Halevy O, Oren M. (1990). *Cell* **62**: 671–680.
Milyavsky M, Shats I, Erez N, Tang X, Senderovich S, Meerson A *et al*. (2003). *Cancer Res* **63**: 7147–7157.
Mirza A, McGuirk M, Hockenberry TN, Wu Q, Ashar H, Black S *et al*. (2002). *Oncogene* **21**: 2613–2622.
Miyashita T, Reed JC. (1995). *Cell* **80**: 293–299.
Murphy M, Ahn J, Walker KK, Hoffman WH, Evans RM, Levine AJ *et al*. (1999). *Genes Dev* **13**: 2490–2501.
Nadav L, Eldor A, Yacoby-Zeevi O, Zamir E, Pecker I, Ilan N *et al*. (2002). *J Cell Sci* **115**: 2179–2187.
O'Doherty U, Swiggard WJ, Malim MH. (2000). *J Virol* **74**: 10074–10080.
Ogishima T, Shiina H, Breault JE, Tabatabai L, Bassett WW, Enokida H *et al*. (2005a). *Clin Cancer Res* **11**: 1028–1036.
Ogishima T, Shiina H, Breault JE, Terashima M, Honda S, Enokida H *et al*. (2005b). *Oncogene* **24**: 6765–6772.
Okamoto K, Beach D. (1994). *EMBO J* **13**: 4816–4822.
Ossovskaya VS, Mazo IA, Chernov MV, Chernova OB, Strezoska Z, Kondratov R *et al*. (1996). *Proc Natl Acad Sci USA* **93**: 10309–10314.
Rohloff J, Zinke J, Schoppmeyer K, Tannapfel A, Witzigmann H, Mossner J *et al*. (2002). *Br J Cancer* **86**: 1270–1275.
Seto E, Usheva A, Zambetti GP, Momand J, Horikoshi N, Weinmann R *et al*. (1992). *Proc Natl Acad Sci USA* **89**: 12028–12032.
Shteper PJ, Zcharia E, Ashhab Y, Peretz T, Vlodavsky I, Ben-Yehuda D. (2003). *Oncogene* **22**: 7737–7749.
Sionov RV, Haupt Y. (1999). *Oncogene* **18**: 6145–6157.
Subbaramaiah K, Altorki N, Chung WJ, Mestre JR, Sampat A, Dannenberg AJ. (1999). *J Biol Chem* **274**: 10911–10915.
Sun Y, Wenger L, Rutter JL, Brinckerhoff CE, Cheung HS. (1999). *J Biol Chem* **274**: 11535–11540.
Timpl R. (1996). *Curr Opin Cell Biol* **8**: 618–624.
Toyoshima M, Nakajima M. (1999). *J Biol Chem* **274**: 24153–24160.
Vlodavsky I, Friedmann Y. (2001). *J Clin Invest* **108**: 341–347.
Vlodavsky I, Friedmann Y, Elkin M, Aingorn H, Atzmon R, Ishai-Michaeli R *et al*. (1999). *Nat Med* **5**: 793–802.
Vlodavsky I, Fuks Z, Bar-Ner M, Ariav Y, Schirrmacher V. (1983). *Cancer Res* **43**: 2704–2711.
Vogelstein B, Lane D, Levine AJ. (2000). *Nature* **408**: 307–310.
Vousden KH, Lu X. (2002). *Nat Rev Cancer* **2**: 594–604.
Weisz L, Zalcenstein A, Stambolsky P, Cohen Y, Goldfinger N, Oren M *et al*. (2004). *Cancer Res* **64**: 8318–8327.
Yoshida M, Kijima M, Akita M, Beppu T. (1990). *J Biol Chem* **265**: 17174–17179.
Zcharia E, Metzger S, Chajek-Shaul T, Friedmann Y, Pappo O, Aviv A *et al*. (2001). *J Mammary Gland Biol Neoplasia* **6**: 311–322.
Zcharia E, Philp D, Edovitsky E, Aingorn H, Metzger S, Kleinman HK *et al*. (2005). *Am J Pathol* **166**: 999–1008.
Zilfou JT, Hoffman WH, Sank M, George DL, Murphy M. (2001). *Mol Cell Biol* **21**: 3974–3985.

Role of endothelial heparanase in delayed-type hypersensitivity

Evgeny Edovitsky, Immanuel Lerner, Eyal Zcharia, Tamar Peretz, Israel Vlodavsky, and Michael Elkin

Heparanase is an endoglycosidase that cleaves heparan sulfate (HS), the main polysaccharide of the basement membrane (BM). HS is responsible for BM integrity and barrier function. Hence, enzymatic degradation of HS in the vascular subendothelial BM is a prerequisite for extravasation of immune cells and plasma components during inflammation. Here, we demonstrate a highly coordinated local heparanase induction upon elicitation of delayed-type hypersensitivity (DTH) reaction in the mouse ear. By monitoring in vivo activation of luciferase gene driven by the heparanase promoter, we demonstrate activation of heparanase transcription at an early stage of DTH. We report that heparanase is produced locally by the endothelium at the site of DTH-associated inflammation. Key DTH mediators, tumor necrosis factor-α and interferon-γ, were found to induce heparanase in cultured endothelial cells. Endothelium emerges as an essential cellular source of heparanase enzymatic activity that, in turn, allows for remodeling of the vascular BM, increased vessel permeability, and extravasation of leukocytes and plasma proteins. In vivo administration of antiheparanase siRNA or an inhibitor of heparanase enzymatic activity effectively halted DTH inflammatory response. Collectively, our results highlight the decisive role of endothelial heparanase in DTH inflammation and its potential as a promising target for anti-inflammatory drug development. (Blood. 2006;107: 3609-3616)

Introduction

Delayed-type hypersensitivity (DTH) is an important in vivo manifestation of cell-mediated immune responses.[1-3] The development of DTH involves recruitment and activation of antigen-specific T cells, synthesis of a cascade of chemotactic and activating cytokines, recruitment of antigen-nonspecific effector cells, fibrin deposition, and increased vascular permeability. This is followed, similar to other types of inflammatory responses, by translocation of leukocytes, including monocytes, neutrophils, and T lymphocytes, from the vascular system, through extracellular tissue barriers, into the site of inflammation.[2-4] Subendothelial basement membrane (BM) represents the major physical obstacle for leukocyte extravasation and entry into inflammatory sites. BM is a specialized type of the extracellular matrix (ECM), underlying endothelial and epithelial cell layers in all tissues and organs. In the blood vessel wall, BM functions as a scaffold for cellular architecture and integrity of the endothelium. Enzymatic remodeling of the BM barrier is a prerequisite for leukocyte extravasation during inflammation. In addition, BM remodeling allows for the extravasation of plasma macromolecules.[3]

The BM is organized as a structural lattice of characteristic protein and polysaccharide constituents. Heparan sulfate glycosaminoglycan represents the principal polysaccharide participating in BM formation.[5-7] Heparan sulfate is composed of repeating disaccharide units that form linear chains covalently bound to a core protein.[8,9] These chains interact through specific attachment sites with the main protein components of BMs, such as collagen IV, laminin, and fibronectin. Such interactions make heparan sulfate an essential molecule responsible for the BM barrier function.[10] The mammalian endoglycosidase heparanase is the predominant enzyme that degrades heparan sulfate.[11-14] Enzymatic cleavage of heparan sulfate results in disassembly of extracellular barriers for cell movement and thus allows for migratory behavior of different cell types in a variety of pathophysiologic conditions, such as morphogenesis, angiogenesis, and cancer metastasis.[11,15-20] Possible involvement of heparanase in inflammation also has been addressed,[4,16,21] emphasizing the contribution of heparanase residing in activated cells of the immune system.[16,21-24] The exact role of heparanase in the inflammatory process remains unclear. Prior to cloning of the heparanase gene, it has been shown that inhibition of T-lymphocyte–derived heparanase by species of heparin inhibits T-cell migration and T-cell–mediated immunity.[21,22,25] The causative involvement of heparanase in this system was questionable, however, because of the multiple biological activities of heparin.[26,27] At the same time, it was reported that degradation products, reportedly released by heparanase from the ECM, inhibit DTH reactivity in mice.[28]

Our research was undertaken to elucidate the source and biological significance of heparanase in inflammation. We applied DTH inflammatory model, as well as recently developed in vivo systems for heparanase overexpression,[29] gene silencing,[30] and

From the Department of Oncology, Hadassah-Hebrew University Medical Center, Jerusalem, and the Cancer and Vascular Biology Research Center, Bruce Rappaport Faculty of Medicine, Technion, Haifa, Israel.

Submitted August 15, 2005; accepted December 19, 2005. Prepublished online as *Blood* First Edition Paper, December 29, 2005; DOI 10.1182/blood-2005-08-3301.

Supported by grants from the United States Army (award no. W81XWH-04-1-0235); the Israel Cancer Association; the European Commission (Fifth Framework program, contract no. QLK3-CT-2002-02049); grant 532/02 from the Israel Science Foundation; and by United States Public Health Service Grant RO1 CA106456-01 from the National Cancer Institute, National Institutes of Health.

Reprints: Israel Vlodavsky, Cancer and Vascular Biology Research Center, Bruce Rappaport Faculty of Medicine, Technion, PO Box 9649, Haifa, 31096, Israel; e-mail: vlodavsk@cc.huji.ac.il; or Michael Elkin, Department of Oncology, Hadassah University Medical Center, POB 12000 Jerusalem 91120, Israel; e-mail: melkin@hadassah.org.il.

The publication costs of this article were defrayed in part by page charge payment. Therefore, and solely to indicate this fact, this article is hereby marked "advertisement" in accordance with 18 U.S.C. section 1734.

monitoring heparanase promoter activation.[31,32] Our results reveal that induction of heparanase gene expression in the vascular endothelium is an important parameter of the inflammatory response. Timely action of endothelial heparanase in the course of inflammation emerges as an essential step, allowing for remodeling of the vascular BM, increased vessel permeability, and extravasation of leukocytes and plasma proteins. A marked decrease in DTH was obtained upon local delivery of antiheparanase siRNA. To our knowledge, this study represents the first successful application of anti-inflammatory therapy based on electroporation-assisted heparanase siRNA delivery in vivo. Given the critical role of heparanase in inflammation and other mechanistically related pathologic processes (ie, tumor progression, angiogenesis),[11,30,33] the anti-heparanase siRNA delivery approach, developed in our study, might be highly relevant to the design of future therapeutic interventions in these conditions.

Materials and methods

Cell culture

Human vascular endothelial EA.Hy926 cells[34,35] were maintained in Dulbecco modified Eagle medium (DMEM) supplemented with 10% fetal calf serum (FCS) and antibiotics at 37°C and 8.5% CO_2. Interferon-γ (IFN-γ) and tumor necrosis factor α (TNFα) were obtained from Sigma (St Louis, MO) and dissolved in water. Prior to treatment with cytokines, cells were maintained for 8 hours in serum-free medium. Then, IFN-γ or TNFα were added for additional 16 hours. Control cultures were treated with the vehicle alone.

RNA isolation and semiquantitative RT-PCR analysis

RNA was isolated with TRIzol (Life Technologies, Grand Island, NY) and quantitated by ultraviolet absorption. Oligo (dT)–primed reverse transcription was performed using 1 μg total RNA in a final volume of 20 μL, and the resulting cDNA was further diluted to 100 μL. Comparative semiquantitative polymerase chain reaction (PCR) was performed as follows: L19 cDNA was first amplified at low cycle number (human L19 primer sequences: L-19-U [5′-ATGCCAACTCTCGTCAACAG-3′] and L-19-L [5′-GCGCTTTCGTGCTTCCTT-3′]). The resulting PCR products were visualized by electrophoresis and ethidium bromide staining, and the intensity of each band was quantified using Scion Image software (Scion, Frederick, MD). If needed, cDNA dilutions were adjusted, and L19 RT-PCR products were re-amplified in order to obtain similar intensities for L19 signals with all the samples. The adjusted amounts of cDNA were used for PCR with primers HPU-355 (TTCGATCCCAAGAAGGAATCAAC) and HPL-229 (GTAGTGATGCCATGTAACTGAATC), designed to amplify a 564-bp PCR product specific for human heparanase.[11] Only RNA samples that gave completely negative results in PCR without reverse transcriptase were further analyzed, to rule out the presence of genomic DNA contamination. Results are expressed as band intensity relative to that of L19 and represent the mean plus or minus standard deviation (SD, indicated by error bars) of 3 independent experiments.

Experimental animals

Female BALB/c mice were purchased from Harlan Laboratories (Jerusalem, Israel). Heparanase-overexpressing transgenic (*hpa*-tg) mice in a C57BL/6J genetic background[29] were bred at the animal facility of the Hadassah-Hebrew University Medical Center. Background genes were tested using C57BL/6J genetic markers. The heparanase transgene was introduced to *hpa*-tg mice under the actin promoter, to drive overexpression of the heparanase gene in most tissues.[29]

Delayed-type hypersensitivity (DTH) assay

DTH reactions were induced in the ear skin of 5- to 6-week-old female BALB/c mice or in *hpa*-transgenic (*hpa*-tg) mice and their wild-type counterparts. Mice were sensitized on the shaved abdominal skin with 100 μL of 2% oxazolone dissolved in acetone/olive oil [4:1 (vol/vol)] applied topically.[28] DTH sensitivity was elicited 5 days later by challenging the mice with 20 μL of 0.5% oxazolone in acetone/olive oil, 10 μL administered topically to each side of the ear. Thickness of a constant area (1 cm^2) of the ear was measured with Mitutoyo engineer's micrometer, immediately before challenging, 24 hours after challenge, and every other day thereafter for 5 days. Five mice were used per each experimental condition and time point, and statistical analysis was performed using the unpaired Student *t* test. The increase in ear thickness over baseline levels (thickness of the ears treated with vehicle alone) was used as a parameter for the extent of inflammation. All experiments were repeated at least twice with similar results.

Immunohistochemistry

Immunohistochemical staining was performed as described[11,32] with minor modifications. Briefly, 5 μm ear tissue sections were incubated in 3% H_2O_2, denatured by boiling (3 minute) in a microwave oven in citrate buffer (0.01 M, pH 6.0), and blocked with 10% goat serum in phosphate-buffered saline (PBS). Sections were incubated with specific polyclonal rabbit antiheparanase antibody (Ab-p3) that was raised against a peptide (R^{273}KTAKMLKSFLKAGGEVI^{290}) corresponding to an internal region of the heparanase 50-kDa subunit[36] and was kindly provided by Dr Robert L. Heinrikson (Pfizer, Kalamazoo, MI). This antibody is cross-reactive with human and mouse heparanase.[32,36] We have also used polyclonal rabbit antiheparanase antibody (733) directed against a synthetic peptide (^{158}KKFKNSTYRSSSVD^{171}) corresponding to the N-terminus of the 50-kDa subunit of the heparanase enzyme.[37] Similar immunostaining pattern was obtained with the 2 antibodies. Color was developed by using the Zymed AEC substrate kit (Zymed Laboratories, San Francisco, CA) for 10 minutes, followed by counterstaining with Mayer hematoxylin. Controls without addition of primary antibody showed low or no background staining in all cases. Slides were visualized with a Zeiss Axioskop 50 microscope (Carl Zeiss, Oberkochen, Germany).

Plasmid constructs and in vivo electroporation

The 1.9-kb human heparanase promoter region (*HPSE* [−1791/+109]-LUC) was subcloned upstream of the luciferase (LUC) gene in a pGL2 basic reporter plasmid (Promega, Madison, WI), as described.[31] Mut-*HPSE*-LUC construct, encoding for the LUC gene under a mutated heparanase promoter sequence, in which deletion was inserted between base pairs −1791/−337, was used as a control. The plasmid containing the LUC gene driven by a cytomegalovirus (CMV) enhancer/promoter (CMV-LUC) was kindly provided by Dr A. Oppenheim (Hadassah Medical Center, Jerusalem, Israel). Antiheparanase siRNA expression vectors were generated as described.[30] The empty pSUPER vector was used as a control.

For in vivo electroporation, mice were anesthetized and plasmid DNA was intradermally injected with a 0.3-mL syringe and 30-gauge needle into the mouse ear (20 μg per site in 25 μL PBS). To keep variability to a minimum, the same skilled operator performed all injections. A 30-second time interval lapsed between injection and initiation of electroporation. The in vivo electroporation system (Genetronics, San Diego, CA) consisted of a square wave pulse generator (ECM 830) and a caliper electrode, applied topically. The caliper electrode (modes 384; BTX/Harvard Apparatus, Holliston, MA) consists of two 1-cm^2 brass plate electrodes. The electroporation was performed by squeezing the ear between the 2 plates and applying 6 pulses of 75 V with a pulse length of 20 msec and interval of 1 second, and polarity reversal after 3 pulses.

Administration of heparanase enzymatic inhibitor ST1514 in vivo

Heparanase inhibitor ST1514 (52% glycol split nonanticoagulant heparin, $H,^{52}$gs, MW = 11 200)[38-40] was kindly provided by Drs Claudio Pisano and Sergio Penco (Sigma-Tau, Pomezia, Rome, Italy). ST1514, or vehicle alone (PBS), were administered intraperitoneally (50 μg/mouse, n = 4 mice/

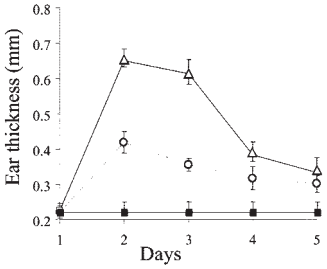

Figure 1. Increased DTH reactivity in heparanase overexpressing transgenic mice. DTH reactions were elicited in the left ear skin of *hpa*-tg mice and their wild-type counterparts using oxazolone. Right ears of the same animals were treated with vehicle alone. Swelling of the challenged ears is expressed in mm as the increase over the baseline thickness measured in ears treated with vehicle alone. Challenged ears in *hpa*-tg mice (△) showed a 3.5-fold increase in swelling over the baseline (■), as compared to only 2-fold increase in wild-type mice (○), 24 hours after challenge with oxazolone. The differences between the 2 groups remained statistically significant for 3 days (n = 5 per experimental condition and time point). Data are expressed as mean ± SD. The experiment was repeated twice with similar results.

group X 2 ears/mice) 1 minute prior to challenge with oxazolone and every hour during the following 8 hours of the experiment.

Permeability assay

DTH challenged (n = 5) and untreated (n = 8) mice received intravenous injections of 100 μL Evans blue dye (30 mg/kg in 100 μL PBS σ) at 16 hours after oxazolone challenge. The intensity of vascular permeability was analyzed macroscopically.

Heparanase activity

Equal protein aliquots of cell lysates from 1×10^6 cells were incubated (3 hours, 37°C, pH 6.6) in dishes coated with ^{35}S-labeled ECM, prepared as described.[11,41] Sulfate-labeled material released into the incubation medium was analyzed by gel filtration on a sepharose 6B column.[41] Nearly intact heparan sulfate proteoglycans are eluted just after the void volume (peak I, $K_{av} < 0.2$, fractions 1-10). Heparan sulfate degradation fragments produced by heparanase are eluted later with $0.5 < K_{av} < 0.8$ (peak II, fractions 15-35).[41] Each experiment was performed at least 3 times, and the variation in elution positions (Kav values) did not exceed 15% of the mean. Reaction buffer with or without recombinant human heparanase (1 ng/mL) was routinely used as a positive or negative control, respectively.

Luciferase assay

Mice ears were removed just before or 48 hours after the DTH challenge with oxazolone. The ears were snap frozen in liquid nitrogen and pulverized to a fine powder with a liquid nitrogen–cooled pestle. The powder was resuspended in 100 μL ice-cold reporter lysis buffer (Promega, Madison, WI), frozen and thawed 3 times, and centrifuged for 20 minutes at 4°C at 20 000*g*. Supernatant was transferred to a new tube, protein content was determined, and 25-μL samples were assayed for LUC activity using the luciferase reporter assay system (Promega). LUC activity was calculated as light units/unit protein, which yields values similar to those based on internal beta-galactosidase transfection standards.[42] Data are presented as the means of at least 3 determinations, and all experiments were repeated at least twice with similar results.

Results

Association between DTH reactivity and heparanase levels

We first studied the DTH reactivity in homozygous transgenic (*hpa*-tg) mice overexpressing human heparanase in all tissues.[29] *Hpa*-tg mice and their wild-type counterparts were sensitized with the hapten oxazolone, as described in "Materials and methods," and the DTH reaction was elicited 5 days later by applying oxazolone onto the ears. Twenty-four hours after the oxazolone challenge, a markedly enhanced inflammatory response and edema formation were detected in *hpa*-tg mice in comparison with wild-type mice, as reflected by a 3.5-fold increase in ear thickness in the *hpa*-tg mice versus a 2-fold increase in wild-type mice (Figure 1). The differences in the extent of edema formation between the 2 groups of mice remained statistically significant for 3 days after challenge (Figure 1). These results prompted us to determine the levels of endogenous heparanase during DTH induction in wild-type mouse ears. As shown in Figure 2B, high levels of the heparanase protein were detected by immunostaining in the ears in which inflammation has been elicited by oxazolone, as compared with low levels or absence of heparanase in control, unchallenged ears (Figure 2A). Notably, a greater part of tissue elements expressing elevated levels of heparanase in the dermis of DTH-affected ears was represented by capillary vascular endothelium (Figure 2B). In the ears of *hpa*-tg mice, both prior to and after challenge, immunostaining revealed elevated heparanase protein content in epithelial keratinocytes (not shown) and vascular endothelial cells (Figure 2C,D). The intensity of heparanase staining in both unchallenged and challenged *hpa*-tg ears was

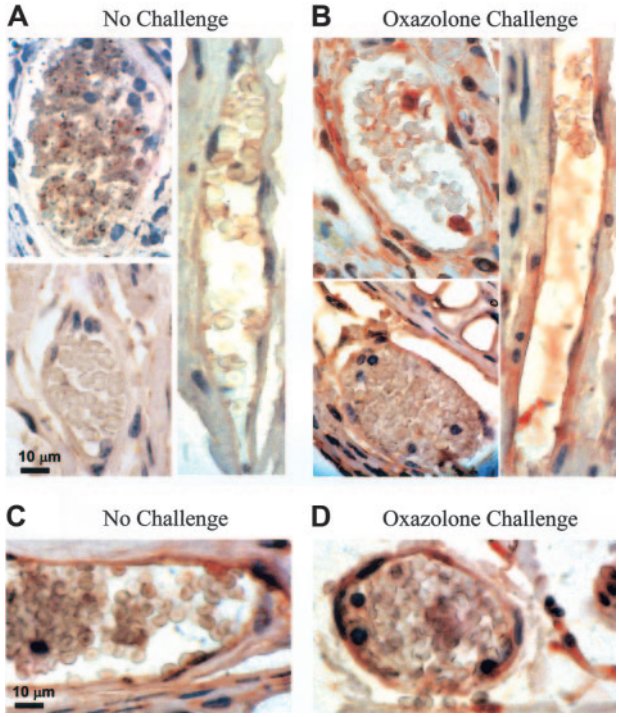

Figure 2. Heparanase expression in vivo upon DTH induction. (A, B) Endogenous heparanase: 5 days after sensitization, left ear (B) of female BALB/c mice (n = 4) was treated with oxazolone and the right ear (A) with vehicle alone. Ear tissues were harvested 24 hours after challenge and processed for immunohistochemical analysis of heparanase expression (reddish staining). Vascular structures were recognized as luminal or slit-like structures that occasionally contained blood cells and were delineated by flattened endothelial cells. This experiment was repeated 3 times, and a similar immunostaining pattern was obtained with 2 different antiheparanase antibodies. Representative microphotographs are shown. (A) Nonchallenged ear: capillary endothelial cells in the ear skin dermis are negative for heparanase staining (magnification × 1000). (B) Oxazolone-challenged ear: heparanase-expressing capillary endothelial cells are easily detected (× 1000). Control sections stained using secondary antibody alone showed no staining. (C, D) When DTH reaction was elicited in *hpa*-tg mice, positive staining was detected in capillary endothelium both prior to (C) and after (D) the challenge. Images were captured with a Zeiss Axioskop 50 microscope (Zeiss, Oberkochen, Germany) equipped with 100 ×/1.30 oil objective or 20 ×/0.50 objective lenses. Images were captured with a Kodak DC290 digital camera (Kodak, Rochester, NY).

similar and comparable to that observed in wild-type animals following the oxazolone challenge (Figure 2B).

Induction of heparanase expression in endothelial cells in vitro by DTH mediator cytokines

Tumor necrosis factor α (TNFα) and interferon γ (IFN-γ) are regarded as key mediators of the DTH reaction.[3,43,44] Stimulatory effect of TNFα on heparanase expression and secretion by the vascular endothelium recently has been reported.[45] We investigated the effect of IFN-γ on endothelial heparanase expression. For this purpose, we used one of the best characterized vascular endothelial cell lines, EA.hy926.[34,35] EA.hy926 cells were treated or untreated with IFN-γ for 24 hours and then tested for heparanase mRNA expression. Semiquantitative reverse transcriptase–polymerase chain reaction (RT-PCR) revealed that IFN-γ treatment yielded a 3-fold increase in heparanase mRNA content, as compared to untreated cells (Figure 3A). Treatment with TNFα yielded a 2-fold increase in heparanase expression by EA.hy926 cells (not shown), in agreement with the previously reported ability of TNFα to augment heparanase expression in other types of endothelial cells.[45] We next determined the levels of heparanase enzymatic activity in EA.hy926 endothelial cells, untreated or treated with IFN-γ, to verify the RT-PCR observations. Heparanase activity was tested by incubation (3 hours, 37°C) of cell lysate samples with a metabolically sulfate-labeled ECM. Sulfate-labeled degradation products released into the incubation medium were subjected to gel filtration on sepharose 6B columns.[11,41] The substrate alone consisted almost entirely of nearly intact, high-molecular-weight material eluted just after the void volume (peak I, fractions 1-10, Kav < 0.2). This material (peak I) has been previously shown to be generated by a proteolytic activity residing in the ECM itself and/or expressed by the cells.[16] The elution pattern of labeled material released during incubation of lysed untreated cells with sulfate-labeled ECM showed little or no heparanase enzymatic activity (Figure 3B). In contrast, a high heparanase activity was detected in lysates of IFN-γ–treated cells, as indicated by a 3- to 4-fold increase in release from ECM of low-molecular-weight sulfate-labeled fragments (peak II, fractions 20-35, $0.5 <$ Kav < 0.8)[11,41] (Figure 3B). These fragments were shown to be degradation products of heparan sulfate, as they were 5- to 6-fold smaller than intact heparan sulfate side chains, resistant to further digestion with papain and chondroitinase ABC, and susceptible to deamination by nitrous acid.[41]

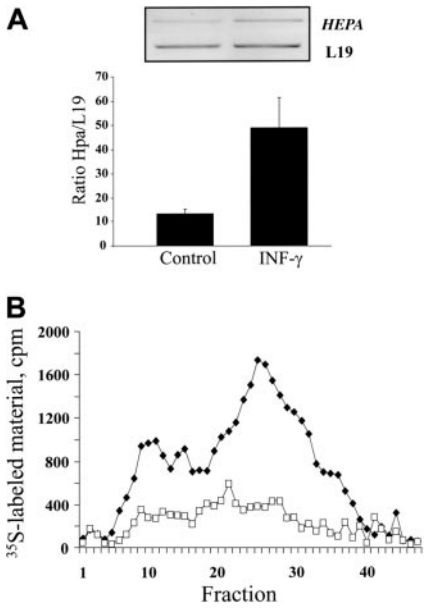

Figure 3. Effects of IFN-γ on heparanase expression in endothelial cells. (A) Semiquantitative RT-PCR. EA.hy926 cells were incubated (16 hours) in triplicate in the absence or presence of 80 ng/mL IFN-γ. RNA was then isolated from the cells, and comparative semiquantitative PCR was performed as described in "Materials and methods." Aliquots (10 μL) of the PCR products were separated by 1.5% agarose gel electrophoresis and visualized (top). The intensity of each band was quantitated using Scion Image software, and the results are expressed as band intensity relative to that of the housekeeping gene L19. The bars represent the mean ± SD (error bars) of 3 independent experiments (bottom). (B) Heparanase activity. EA.hy926 cells were incubated (16 hours) in the absence (□), or presence (♦) of 80 ng/mL IFN-γ. Cell lysates were normalized for equal protein and incubated (3 hours, pH 6.0, 37°C) with sulfate-labeled ECM. Labeled degradation fragments released into the incubation medium were analyzed by gel filtration on sepharose 6B.

Heparanase promoter activation during DTH inflammation

In order to test whether heparanase induction during inflammation occurs due to a transcriptional activation of the heparanase gene, we next applied the in vivo electroporation technique, based on injection of the expression vector into the ear, followed by application of an electric field[32,46] to deliver the LUC reporter gene driven by the heparanase promoter (Hpse-LUC)[31] into the ear, prior to DTH elicitation. Four days following sensitization with oxazolone, the ears of BALB/c mice in the experimental group were electroporated with the *HPSE*-LUC construct. Ears of mice in the control group were electroporated with construct containing the LUC gene under a constitutive CMV promoter (CMV-LUC).[32] In an additional control group, ears of mice were electroporated with a construct containing the LUC gene driven by a mutated heparanase promoter, bearing a deletion between base pairs −1791 and −337 (Mut-*HPSE*-LUC). Twenty-four hours later, left ears of the mice in experimental and both control groups were challenged with oxazolone, while the right ears were left untreated. Forty-eight hours after challenge, when a strong DTH-associated swelling was readily detected in all ears challenged with oxazolone, but not in nonchallenged ears (not shown), the mice were killed and the ears removed, snap frozen, and lysed. Samples were normalized for total protein content and luciferase activity was measured as described in "Materials and methods." As shown in Figure 4A, DTH induction in left ears provoked a marked activation of the heparanase promoter, yielding a 23-fold increase ($P < .003$) in LUC activity measured in left (DTH) versus right (control) ears of mice from the experimental group. In contrast, in the ears of mice electroporated with a CMV-LUC construct, DTH induction did not result in any statistically significant change in LUC activity (Figure 4B), while no LUC activity was detected in either left (DTH) or right (control) ears of mice electroporated with the Mut-*HPSE*-LUC construct (Figure 4C), verifying that the difference observed in the experimental group was heparanase promoter–specific and not due to variation in transfection efficiency. These data indicate that the increase in heparanase levels in DTH inflammation occurs through specific activation of the heparanase gene promoter.

Local silencing of heparanase profoundly decreases inflammatory response in vivo

To explore the effect of local heparanase silencing on DTH reactivity, we delivered anti–mouse heparanase siRNA (pSi2) expression vector[30] to BALB/c mouse ears 24 hours prior to challenge with the hapten. The design of the pSi2 vector and demonstration of its knock-down effect on mouse heparanase gene expression (80% inhibition) in cultured cells have been previously described by us.[30] In the present study, we applied an in vivo

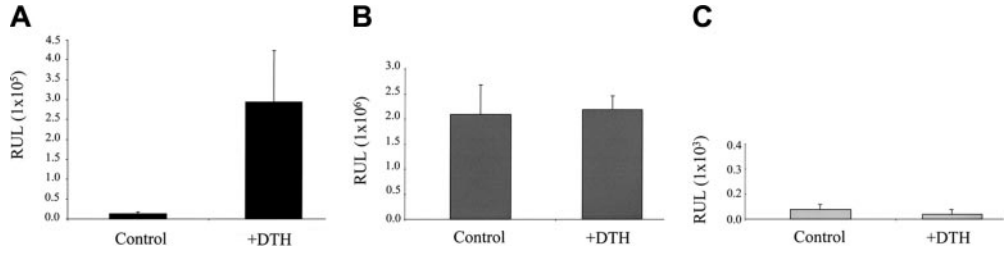

Figure 4. Heparanase promoter is activated upon DTH elicitation. The ears of oxazolone-sensitized BALB/c mice (n = 3) were electroporated with Hpse-LUC (A, experimental group), CMV-LUC (B, control group), or Mut-Hpse-LUC (C, control group) reporter constructs. Left ears in both the experimental and control groups were challenged 24 hours later, while right ears remained untreated. Forty-eight hours after challenge, when a pronounced DTH reaction was noted in the left, but not right, ears of all mice (as judged by ear swelling and edema formation), the ears were resected, snap frozen, and lysed. Lysates were normalized for total protein content. Luciferase activity was determined as described in "Materials and methods" and expressed in relative units of light (RUL). Two independent experiments were performed, 3 mice per treatment.

electroporation technique, as described in "Materials and methods." To demonstrate that this technique ensures actual delivery of the electroporated DNA and its uniform expression in the ear tissue, we first electroporated the ears of male BALB/c mice with a CMV-LUC construct, encoding for luciferase gene under the constitutive CMV promoter, and visualized the expression of luciferase in the mouse ears in vivo (Figure 5C), using a cooled charged coupled device (CCCD) camera.[32]

In the subsequent set of experiments, 6-week-old male BALB/c mice were sensitized with oxazolone and divided into 3 groups (n = 5 mice per group) 4 days after sensitization. The first and second groups were electroporated with antiheparanase siRNA expression vector (pSi2) and with empty vector (pSUPER),[47] respectively; mice in the third group were not subjected to electroporation. Twenty-four hours later, ears in all 3 groups were challenged with the hapten. Hapten also was applied onto the ears of an additional 5 mice, which had not been previously sensitized or electroporated, serving as a negative control group. The ear thickness was monitored for 5 consecutive days (Figure 5A). Twenty-four hours after challenge, a marked inflammatory response was detected in both the pSUPER-electroporated and nonelectroporated ears, reflected by more than a 2-fold increase in ear thickness, as compared with the control group. In contrast, in the ears electroporated with the antiheparanase siRNA encoding vector pSi2, the inflammatory response was significantly inhibited, as noted by a 77% decrease in ear swelling and edema formation, compared to ears electroporated with the pSUPER vector alone (Figure 5A). We previously have demonstrated the persistence of heparanase silencing in murine cells in vitro following pSi2 transfection (75% inhibition at 48 hours after transfection and 50% inhibition at 96 hours after transfection). To test inhibitory effect of siRNA silencing in endothelial cells, we determined heparanase activity in human EA.hy926 vascular endothelial cells at various time points after electroporation with the anti–human heparanase siRNA encoding pSH1 vector, analogous to pSi2. Maximal effect of siRNA silencing (80% inhibition) was observed during the first 72 hours after electroporation and was still pronounced by 96 hours after electroporation (50% inhibition, not shown). To test the local heparanase expression in siRNA-treated skin and to ensure that electroporation of pSi2 resulted in heparanase silencing throughout the in vivo experiment, we compared heparanase immunostaining in tissue sections of the ears in which DTH was induced following

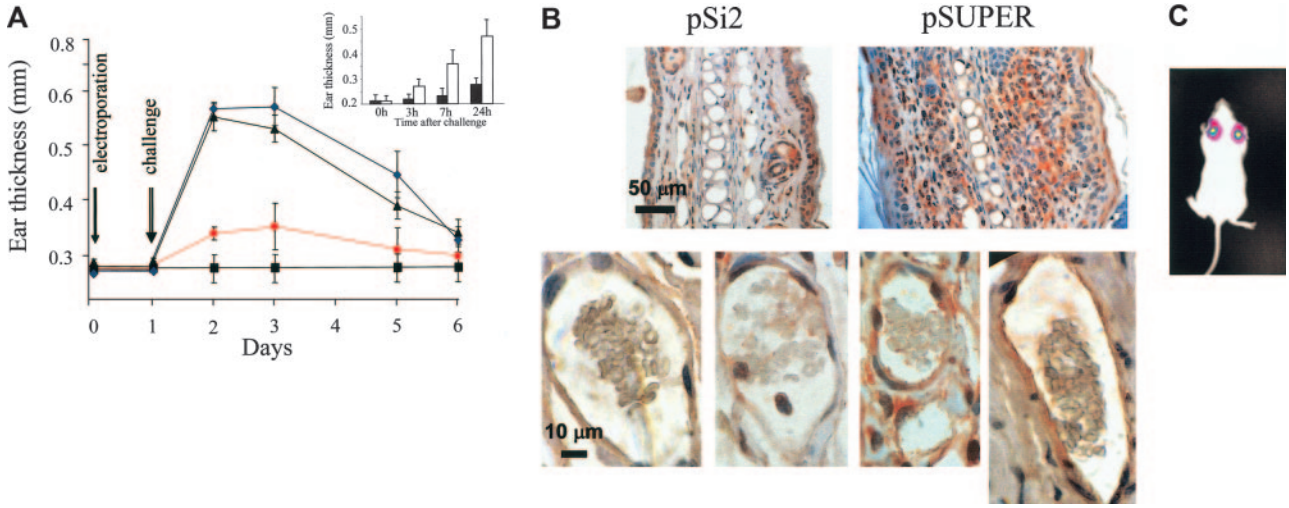

Figure 5. Effect of antiheparanase siRNA on DTH reactivity in vivo. Ears of oxazolone-sensitized BALB/c mice were electroporated with anti–mouse heparanase siRNA expression vector pSi2 (●); empty vector pSUPER (▲); or received no plasmid or electroporation (◆), followed by challenge with the hapten 24 hours later. Hapten also was applied on the ears of 5 additional mice, which have not been previously sensitized or electroporated (■). Three independent experiments were performed, and 5 mice per treatment were used. (A) Ear thickness was measured for 5 consecutive days after challenge. Inset. Effect of treatment with an inhibitor (ST1514) of heparanase enzymatic activity on DTH reactivity. ST1514 or vehicle alone was administered intraperitoneally prior to challenge and every hour thereafter (50 μg/injection) during the following 8 hours of the experiment. Filled bars: ear thickness in ST1514-treated mice; empty bars: ear thickness in vehicle-treated mice. (B) The ears in which DTH was induced following electroporation with pSi2 (left) or pSUPER (right) vectors were harvested 48 hours after challenge and processed for immunohistochemical analysis of heparanase expression (reddish staining; sebaceous glands are positively stained in all preparates, due to nonspecific absorption, as previously reported.[32] Top: magnification × 200; bottom: × 1000. Positively stained capillary endothelium is noted in the dermis of pSUPER but not pSi2-electroporated ear skin. (C) To demonstrate that electroporation ensures the actual delivery of plasmid DNA and its uniform expression in the ear tissue, the ears of male BALB/c mice were electroporated with a CMV-LUC construct, encoding for luciferase gene under the constitutive CMV promoter. Expression of luciferase in the mouse ears in vivo was monitored as described in "Materials and methods."[32]

electroporation with the pSi2 or pSUPER vectors. Intense heparanase staining was observed in pSUPER-electroporated ears, 48 hours after the challenge (that is, 72 hours after electroporation, Figure 5B, right), versus a very weak or no heparanase staining in pSi2-electroporated ears (Figure 5B, left), similar to heparanase levels observed in normal untreated ears (Figure 2A). Decrease in a number of positively stained cells other than endothelial cells (ie, epidermal and hair follicle keratinocytes, several dermis-residing cells that may express basal levels of heparanase[32,39]) also was found in pSi2-electroporated ears (Figure 5B, left). Altogether, these results demonstrate that heparanase gene silencing in pSi2-electroporated ears persisted at least for 2 days following the challenge.

We next tested the effect of the potent heparanase enzymatic inhibitor ST1514 (glycol split, nonanticoagulant heparin[38-40]) on DTH reactivity. Six-week-old male BALB/c mice were sensitized with oxazolone and divided into 2 groups (n = 4 mice per group × 2 ears) 4 days after sensitization. The first group was treated with ST1514 immediately prior to challenge and every hour thereafter during the following 8 hours of the experiment, as described in "Materials and methods." The second group was treated with vehicle alone. Treatment with ST1514 resulted in a significant decrease of ear swelling and edema formation, as compared to treatment with the vehicle (Figure 5A, inset), further verifying the involvement of heparanase in DTH and the relevance of heparanase inhibition as an anti-inflammatory approach.

Heparanase silencing inhibits vessel permeability during DTH

Since we found reduced inflammatory response (reflected by a very limited ear swelling) following heparanase silencing in wild-type mice, as well as increased edema formation in *hpa*-tg mice, we next investigated whether heparanase directly affects vascular leakage, a hallmark of the early phase of inflammation. The ears of oxazolone-sensitized BALB/c mice were electroporated with pSi2- (left ear) or pSUPER- (right ear) vectors on day 4 after sensitization. Twenty-four hours later, both the right and left ears were challenged with oxazolone, and after an additional 16 hours mice received intravenous injections of Evans blue. As shown in Figure 6, 16.5 hours after DTH elicitation by oxazolone challenge, vascular leakage was significantly higher in pSUPER- than in pSi2-electroporated ears, as reflected by a marked difference in Evans blue extravasation. Macroscopically, a strong DTH-associated swelling was readily detected in all pSUPER-, but not in pSi2-electroporated ears (not shown). These findings indicate that increased heparanase activity expressed by activated endothelial cells at the site of inflammation enables vessel leakage during inflammation, most likely due to damage and disruption of the subendothelial BM.

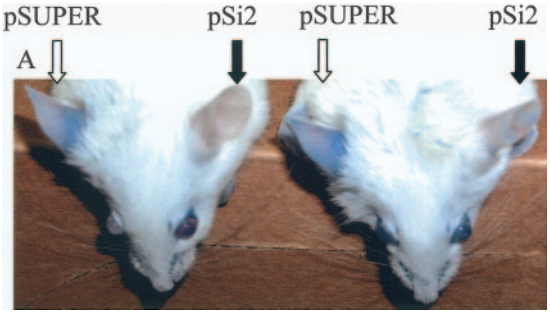

Figure 6. Effect of local heparanase silencing on vascular leakage. Ears of 5 oxazolone-sensitized BALB/c mice were electroporated with either antiheparanase siRNA pSi2 (filled arrows) or empty pSUPER (empty arrows) vectors, 24 hours prior to induction of DTH reaction by application of oxazolone onto the ears of both sides. Evans blue dye was injected intravenously 16 hours later. Unlike the massive Evans blue extravasation observed in pSUPER-electroporated ears, pSi2 electroporation halted vascular leakage, as visualized by the near absence of extravasated Evans blue dye.

Discussion

Contrary to early considerations, endothelial cells are now recognized as active participants in DTH reactivity and other types of inflammatory processes.[3,48,49] Following alterations induced by pro-inflammatory cytokines (ie, TNFα, IFN-γ) acting in concert, endothelial cells become activated and synthesize numerous adhesion molecules involved in leukocyte-endothelium interactions.[3] Endothelial cells also are capable of secreting different molecules (ie, cytokines, chemokines) that attract various types of immune cells into the site of inflammation and increase the motility of adherent leukocytes from the peripheral blood. Moreover, endothelial cells were proposed to contribute to local vessel hyperpermeability by remodeling the subendothelial BM and thus allowing the extravasation of plasma macromolecules (eg, fibrinogen) and immunocytes. However, attempts to identify the molecular mechanism responsible for increased vascular permeability in DTH inflammation were met with limited success. The data presented in this study directly implicate the heparanase enzyme, locally expressed by the vascular endothelium at the site of inflammation, in degradation of the subendothelial BM and subsequent vascular leakage—a hallmark of delayed hypersensitivity skin reactions.[1]

Mammalian heparanase cleaves heparan sulfate glycosaminoglycans in the BM and other types of ECM.[11,50] Given the essential role of heparan sulfate chains in preserving the integrity and barrier properties of the BM and ECM,[8-10,51] heparanase may adversely affect tissue architecture and play an important role in processes that involve ECM disintegration, such as implantation, morphogenesis, angiogenesis, and cancer metastasis.[10,11,29,33,50,52,53]

Less is known about the role of heparanase in inflammation. It was reported that polyanionic compounds known to inhibit heparanase enzymatic activity (eg, heparin) also inhibit inflammatory responses.[21,25,54,55] Activated T lymphocytes have been viewed as a cellular source of the enzyme in inflammation.[16,21,22,24,55] On the other hand, it was found that the ability of lymphocytes to degrade ECM is inhibited by key inflammatory cytokines.[56]

Here, we demonstrated the induction of locally expressed heparanase at the site of inflammation in vivo and established its mechanistic involvement in DTH inflammatory reaction. Overexpression of heparanase in a mouse transgenic model significantly enhanced DTH reactivity. Unlike the intensity of the DTH reaction, its time course remained the same in both transgenic and wild-type animals (Figure 1). This suggests that heparanase is involved primarily in the initial stages of the inflammatory response, that is, increase in vascular permeability, most likely through disruption of the subendothelial BM. By monitoring in vivo activity of luciferase driven by the heparanase gene regulatory sequence, we demonstrated that heparanase promoter activation occurs in the inflammation site upon the onset of a DTH response. Studying expression and cellular distribution of endogenous heparanase in BALB/c mice, we found that endothelial cells are the primary source of the enzyme at the early stages of DTH inflammation. Furthermore, TNFα and IFN-γ, key mediators of DTH inflammation,[3,43,44] up-regulate heparanase gene expression and increase heparanase enzymatic activity in cultured endothelial cells. Our data on

heparanase induction by TNFα are in agreement with the previously reported ability of TNFα to augment ECM degradation by endothelial cells[56] and are consistent with a recent report by Chen et al.[45] In the latter study, caspase 8 was identified as a part of a molecular pathway that underlies TNFα-induced heparanase secretion by endothelial cells. The molecular mechanism through which IFNγ augments heparanase expression remains to be further investigated. Computerized analysis of the heparanase gene 1.9-kb regulatory sequence using MatInspector software[57] revealed 2 interferon-stimulated response elements (ISREs) consensus sequences in the promoter region that specifically bind transcription factors activated by interferon (not shown). A more refined analysis of the heparanase regulatory sequence will enable researchers to locate the precise binding site(s) in the heparanase promoter responsible for the IFN-γ–induced transcription.

Local in vivo electroporation of antiheparanase siRNA into the ear skin markedly inhibited DTH reactivity, demonstrating the decisive involvement of heparanase in inflammation. In order to distinguish between heparanase expressed by local cellular elements at the site of inflammation versus the enzyme expressed by circulating immunocytes, the in vivo siRNA experiments were designed to achieve heparanase silencing 1 day prior to challenge with the hapten. Since T cells, known to mediate DTH response, attach to the vascular endothelium and extravasate toward the hapten only after the challenge,[2] we did not expose the recruited T cells to antiheparanase siRNA administered by local electroporation executed prior to challenge. The same is correct for any other free circulating cells of the immune system. On the other hand, endothelial cells are present at the challenged site before application of the hapten. Thus, unlike systemic administration of heparanase-inhibiting compound ST1514, treatment with siRNA prior to challenge restricted heparanase silencing to the local (eg, endothelium), rather than circulating (eg, T lymphocytes) cellular compartment. Although not capable of fully discriminating between the heparanase producer cell types, this approach allowed us to specifically analyze the role of nonlymphocyte-derived heparanase in inflammation. The decrease in heparanase protein, observed in the endothelium of immunostained ear tissue derived from pSi2-treated ears (Figure 5B), demonstrated the effectiveness of heparanase silencing in vivo. This decrease correlated with the absence of vessel leakage (Figure 6), as compared to control pSUPER-treated ears, in which vessel hyperpermeability and ear swelling were clearly noted. In summary, induction of locally expressed heparanase emerges as an important step in the series of events involved in onset of the DTH inflammatory process. Our results suggest that following hapten challenge, induction of heparanase expression driven by inflammatory cytokines (TNFα and, later on, IFN-γ) may occur locally in the endothelial cells. Upon elicitation of DTH reaction, TNFα (ie, released via mast cells' degranulation in response to hapten challenge[44]) may induce initial increase in production and secretion of heparanase by endothelial cells (this study and Chen et al[45]). At this stage, heparanase, known to promote cell adhesion,[58] can improve T-cell adherence to the endothelium, as well as facilitate extravasation, through degradation of the subendothelial basement membrane. Then, IFN-γ released by the extravasated T cells may contribute to preservation and even further amplification of heparanase expression in the endothelium. Continuous increase in heparanase levels is likely to cause vascular leakage through degradation of HS chains, responsible for the structural integrity of the subendothelial BM. Such degradation results in disruption of the BM permeaselective properties and subsequent plasma and immunocyte extravasation. Disruption of the BM due to elevated heparanase levels has been demonstrated in *hpa*-tg mouse mammary epithelium.[29] HS proteoglycans (ie, syndecans) also are present on the surface of endothelial cells and have been shown to modulate vascular permeability and leukocyte trafficking in inflammation.[59] Thus, the observed effects of heparanase may, in addition to cleavage of BM-residing HS, be due to degradation of endothelial cell surface HS chains, impairing their barrier function. To our knowledge, these data represent the first successful in vivo application of heparanase siRNA-based anti-inflammatory therapy. Heparanase inhibition may be relevant in the development of future therapeutic tools in several disorders considered to be the consequence of DTH reactions such as rheumatoid arthritis, psoriasis, and inflammatory bowel disease (IBD). In particular, preferential expression of heparanase in the intestinal tissue of IBD patients, as well as increased susceptibility of *hpa*-tg mice to chemically-induced colitis (Y. Sherman, I.L., M.E., I.V., unpublished results, May 2005), attest to heparanase as a likely target for the design of a novel anti-IBD treatment.

Previously, we showed that heparanase gene silencing approach applied in vitro specifically suppresses invasive and metastatic potential in various tumor models.[30] Thus, in addition to the potential promise for an anti-inflammatory treatment, the specific heparanase siRNA delivery system described in this study will encourage development of novel heparanase-based therapeutic modalities, highly pertinent in other pathological conditions involving undesired heparanase activity, particularly cancer.[60-63]

Acknowledgments

We would like to thank Dr T. San (Department of Oncology, Hadassah University Hospital) for the excellent technical support and Dr S. Frankenburg (Department of Dermatology, Hadassah University Hospital) for fruitful discussions and for help in establishing the DTH model. We thank Drs Claudio Pisano and Sergio Penco (Sigma-Tau Research Department, Pomezia, Rome, Italy) and Prof Benito Casu ("Ronzoni" Institute, Milan, Italy) for kindly providing the ST1514 glycol-split heparin and for their continuous support.

References

1. Voisin GA, Toullet F. Studies on hypersensitivity, I: demonstration and description of an increase of vascular permeability in the tuberculin hypersensitivity reactions. Ann Inst Pasteur. 1963;104:169-196.
2. Abbas AK. Cell-mediated (type IV) hypersensitivity. In: Kumar V, Abbas AK, Fausto N, eds. Pathologic Basis of Disease. 7th ed. Philadelphia, PA: Elsevier Saunders; 2005:216-217.
3. Black CA. Delayed type hypersensitivity: current theories with an historic perspective. Dermatol Online J. 1999;5:7.
4. Vaday GG, Lider O. Extracellular matrix moieties, cytokines, and enzymes: dynamic effects on immune cell behavior and inflammation. J Leukoc Biol. 2000;67:149-159.
5. Noonan DM, Fulle A, Valente P, et al. The complete sequence of perlecan, a basement membrane heparan sulfate proteoglycan, reveals extensive similarity with laminin A chain, low density lipoprotein-receptor, and the neural cell adhesion molecule. J Biol Chem. 1991;266: 22939-22947.
6. Timpl R. Proteoglycans of basement membranes. Experientia. 1993;49:417-428.
7. Iozzo RV, Murdoch AD. Proteoglycans of the extracellular environment: clues from the gene and protein side offer novel perspectives in molecular diversity and function. FASEB J. 1996;10:598-614.
8. Timpl R. Macromolecular organization of basement membranes. Curr Opin Cell Biol. 1996;8: 618-624.
9. Bernfield M, Gotte M, Park PW, et al. Functions of

cell surface heparan sulfate proteoglycans. Annu Rev Biochem. 1999;68:729-777.

10. Vlodavsky I. Involvement of the extracellular matrix, heparan sulfate proteoglycans, and heparan sulfate degrading enzymes in angiogenesis and metastasis. In: Bicknell LC, Ferrara N, eds. Tumour Angiogenesis. Oxford, United Kingdom. Oxford University Press; 1997:125-140.
11. Vlodavsky I, Friedmann Y, Elkin M, et al. Mammalian heparanase: gene cloning, expression and function in tumor progression and metastasis. Nat Med. 1999;5:793-802.
12. Hulett MD, Freeman C, Hamdorf BJ, Baker RT, Harris MJ, Parish CR. Cloning of mammalian heparanase, an important enzyme in tumor invasion and metastasis. Nat Med. 1999;5:803-809.
13. Kussie PH, Hulmes JD, Ludwig DL, et al. Cloning and functional expression of a human heparanase gene. Biochem Biophys Res Commun. 1999;261:183-187.
14. Toyoshima M, Nakajima M. Human heparanase: purification, characterization, cloning, and expression. J Biol Chem. 1999;274:24153-24160.
15. Vlodavsky I, Bar-Shavit R, Ishai-Michaeli R, Bashkin P, Fuks Z. Extracellular sequestration and release of fibroblast growth factor: a regulatory mechanism? Trends Biochem Sci. 1991;16: 268-271.
16. Vlodavsky I, Eldor A, Haimovitz-Friedman A, et al. Expression of heparanase by platelets and circulating cells of the immune system: possible involvement in diapedesis and extravasation. Invasion Metastasis. 1992;12:112-127.
17. Vlodavsky I, Mohsen M, Lider O, et al. Inhibition of tumor metastasis by heparanase inhibiting species of heparin. Invasion Metastasis. 1994;14: 290-302.
18. Vlodavsky I, Friedmann Y. Molecular properties and involvement of heparanase in cancer metastasis and angiogenesis. J Clin Invest. 2001;108: 341-347.
19. Nakajima M, Irimura T, Nicolson GL. Heparanases and tumor metastasis. J Cell Biochem. 1988;36:157-167.
20. Parish CR, Freeman C, Hulett MD. Heparanase: a key enzyme involved in cell invasion. Biochim Biophys Acta. 2001;1471:M99-M108.
21. Lider O, Mekori YA, Miller T, et al. Inhibition of T lymphocyte heparanase by heparin prevents T cell migration and T cell–mediated immunity. Eur J Immunol. 1990;20:493-499.
22. Lider O, Baharav E, Mekori YA, et al. Suppression of experimental autoimmune diseases and prolongation of allograft survival by treatment of animals with low doses of heparins. J Clin Invest. 1989;83:752-756.
23. Matzner Y, Bar-Ner M, Yahalom J, Ishai-Michaeli R, Fuks Z, Vlodavsky I. Degradation of heparan sulfate in the subendothelial extracellular matrix by a readily released heparanase from human neutrophils: possible role in invasion through basement membranes. J Clin Invest. 1985;76: 1306-1313.
24. Fridman R, Lider O, Naparstek Y, Fuks Z, Vlodavsky I, Cohen IR. Soluble antigen induces T lymphocytes to secrete an endoglycosidase that degrades the heparan sulfate moiety of subendothelial extracellular matrix. J Cell Physiol. 1987; 130:85-92.
25. Sy MS, Schneeberger E, McCluskey R, Greene MI, Rosenberg RD, Benacerraf B. Inhibition of delayed-type hypersensitivity by heparin depleted of anticoagulant activity. Cell Immunol. 1983;82: 23-32.
26. Koenig A, Norgard-Sumnicht K, Linhardt R, Varki A. Differential interactions of heparin and heparan sulfate glycosaminoglycans with the selectins: implications for the use of unfractionated and low molecular weight heparins as therapeutic agents. J Clin Invest. 1998;101:877-889.
27. Borsig L, Wong R, Feramisco J, Nadeau DR, Varki NM, Varki A. Heparin and cancer revisited: mechanistic connections involving platelets, P-selectin, carcinoma mucins, and tumor metastasis. Proc Natl Acad Sci U S A. 2001;98:3352-3357.
28. Lider O, Cahalon L, Gilat D, et al. A disaccharide that inhibits tumor necrosis factor alpha is formed from the extracellular matrix by the enzyme heparanase. Proc Natl Acad Sci U S A. 1995;92: 5037-5041.
29. Zcharia E, Metzger S, Chajek-Shaul T, et al. Transgenic expression of mammalian heparanase uncovers physiological functions of heparan sulfate in tissue morphogenesis, vascularization, and feeding behavior. FASEB J. 2004;18:252-263.
30. Edovitsky E, Elkin M, Zcharia E, Peretz T, Vlodavsky I. Heparanase gene silencing, tumor invasiveness, angiogenesis, and metastasis. J Natl Cancer Inst. 2004;96:1219-1230.
31. Elkin M, Cohen I, Zcharia E, et al. Regulation of heparanase gene expression by estrogen in breast cancer. Cancer Res. 2003;63:8821-8826.
32. Zcharia E, Philp D, Edovitsky E, et al. Heparanase regulates murine hair growth. Am J Pathol. 2005;166:999-1008.
33. Elkin M, Ilan N, Ishai-Michaeli R, et al. Heparanase as mediator of angiogenesis: mode of action. FASEB J. 2001;15:1661-1663.
34. Edgell CJ, McDonald CC, Graham JB. Permanent cell line expressing human factor VIII–related antigen established by hybridization. Proc Natl Acad Sci U S A. 1983;80:3734-3737.
35. Bouis D, Hospers GA, Meijer C, Molema G, Mulder NH. Endothelium in vitro: a review of human vascular endothelial cell lines for blood vessel–related research. Angiogenesis. 2001;4:91-102.
36. Fairbanks MB, Mildner AM, Leone JW, et al. Processing of the human heparanase precursor and evidence that the active enzyme is a heterodimer. J Biol Chem. 1999;274:29587-29590.
37. Zetser A, Levy-Adam F, Kaplan V, et al. Processing and activation of latent heparanase occurs in lysosomes. J Cell Sci. 2004;117:2249-2258.
38. Naggi A, Casu B, Perez M, et al. Modulation of the heparanase-inhibiting activity of heparin through selective desulfation, graded N-acetylation, and glycol splitting. J Biol Chem. 2005;280: 12103-12113.
39. Zcharia E, Zilka R, Yaar A, et al. Heparanase accelerates wound angiogenesis and wound healing in mouse and rat models. FASEB J. 2005;19: 211-221.
40. Casu B, Guerrini M, Guglieri S, et al. Undersulfated and glycol-split heparins endowed with antiangiogenic activity. J Med Chem. 2004;47:838-848.
41. Vlodavsky I, Fuks Z, Bar-Ner M, Ariav Y, Schirrmacher V. Lymphoma cell-mediated degradation of sulfated proteoglycans in the subendothelial extracellular matrix: relationship to tumor cell metastasis. Cancer Res. 1983;43:2704-2711.
42. Nawaz Z, Stancel GM, Hyder SM. The pure antiestrogen ICI 182780 inhibits progestin-induced transcription. Cancer Res. 1999;59:372-376.
43. Fong TA, Mosmann TR. The role of IFN-gamma in delayed-type hypersensitivity mediated by Th1 clones. J Immunol. 1989;143:2887-2893.
44. Rocken M, Hultner L. Heavy functions for light chains. Nat Med. 2002;8:668-670.
45. Chen G, Wang D, Vikramadithyan R, et al. Inflammatory cytokines and fatty acids regulate endothelial cell heparanase expression. Biochemistry. 2004;43:4971-4977.
46. Zhang L, Nolan E, Kreitschitz S, Rabussay DP. Enhanced delivery of naked DNA to the skin by non-invasive in vivo electroporation. Biochim Biophys Acta. 2002;1572:1-9.
47. Brummelkamp TR, Bernards R, Agami R. A system for stable expression of short interfering RNAs in mammalian cells. Science. 2002;296: 550-553.
48. Sana TR, Janatpour MJ, Sathe M, McEvoy LM, McClanahan TK. Microarray analysis of primary endothelial cells challenged with different inflammatory and immune cytokines. Cytokine. 2005; 29:256-269.
49. Standage BA, Vetto RM, Jones R, Burger DR. Vascular endothelial cells in cell-mediated immunity: adoptive transfer with in vitro conditioned cells is genetically restricted at the endothelial cell barrier. J Cell Biochem. 1985;29:45-56.
50. Vlodavsky I, Goldshmidt O, Zcharia E, et al. Molecular properties and involvement of heparanase in cancer progression and normal development. Biochimie. 2001;83:831-839.
51. Kalluri R. Basement membranes: structure, assembly and role in tumor angiogenesis. Nat Rev Cancer. 2003;3:422-433.
52. Goldshmidt O, Zcharia E, Aingorn H, et al. Expression pattern and secretion of human and chicken heparanase are determined by their signal peptide sequence. J Biol Chem. 2001;276: 29178-29187.
53. Goldshmidt O, Zcharia E, Abramovitch R, et al. Cell surface expression and secretion of heparanase markedly promote tumor angiogenesis and metastasis. Proc Natl Acad Sci U S A. 2002;99: 10031-10036.
54. Kakakios AM, Ryan J, Geczy CL. Effect of locally administered heparins on delayed-type hypersensitivity reactions. Int Arch Allergy Appl Immunol. 1990;93:300-307.
55. Parish CR, Coombe DR, Jakobsen KB, Bennett FA, Underwood PA. Evidence that sulphated polysaccharides inhibit tumor metastasis by blocking tumor-cell–derived heparanases. Int J Cancer. 1987;40:511-518.
56. Bartlett MR, Underwood PA, Parish CR. Comparative analysis of the ability of leucocytes, endothelial cells and platelets to degrade the subendothelial basement membrane: evidence for cytokine dependence and detection of a novel sulfatase. Immunol Cell Biol. 1995;73:113-124.
57. Quandt K, Frech K, Karas H, Wingender E, Werner T. MatInd and MatInspector: new fast and versatile tools for detection of consensus matches in nucleotide sequence data. Nucleic Acids Res. 1995;23:4878-4884.
58. Goldshmidt O, Zcharia E, Cohen M, et al. Heparanase mediates cell adhesion independent of its enzymatic activity. FASEB J. 2003;17:1015-1025.
59. Gotte M. Syndecans in inflammation. FASEB J. 2003;17:575-591.
60. Gohji K, Okamoto M, Kitazawa S, et al. Heparanase protein and gene expression in bladder cancer. J Urol. 2001;166:1286-1290.
61. Friedmann Y, Vlodavsky I, Aingorn H, et al. Expression of heparanase in normal, dysplastic, and neoplastic human colonic mucosa and stroma: evidence for its role in colonic tumorigenesis. Am J Pathol. 2000;157:1167-1175.
62. Maxhimer JB, Quiros RM, Stewart R, et al. Heparanase-1 expression is associated with the metastatic potential of breast cancer. Surgery. 2002;132:326-333.
63. Koliopanos A, Friess H, Kleeff J, et al. Heparanase expression in primary and metastatic pancreatic cancer. Cancer Res. 2001;61:4655-4659.